

# Activity-Dependent Initiation of a Prolonged Depolarization in *Aplysia* Bag Cell Neurons: Role for a Cation Channel

Anne Y. Hung and Neil S. Magoski

Department of Physiology, Queen's University, Kingston, Ontario, Canada

Submitted 6 September 2006; accepted in final form 17 January 2007

**Hung AY, Magoski NS.** Activity-dependent initiation of a prolonged depolarization in *Aplysia* bag cell neurons: role for a cation channel. *J Neurophysiol* 97: 2465–2479, 2007; doi:10.1152/jn.00941.2006. The translation of prior activity into changes in excitability is essential for memory and the initiation of behavior. After brief synaptic input, the bag cell neurons of *Aplysia californica* undergo a nearly 30-min afterdischarge to release egg-laying hormone. The present study examines a prolonged depolarization in cultured bag cell neurons. A 5-Hz, 10-s action potential train elicited a depolarization of about 10 mV, which lasted  $\leq 30$  min and was reduced by calmodulin kinase inhibition. Very broad action potentials (resulting from TEA application) decreased prolonged depolarization amplitude, indicating that strong  $\text{Ca}^{2+}$  influx did not necessarily promote the response. The prolonged depolarization current ( $I_{\text{PD}}$ ) was recorded after 5-Hz, 10-s trains of square voltage pulses of varying duration (10–150 ms). Despite  $\text{Ca}^{2+}$  influx increasing steadily with pulse duration,  $I_{\text{PD}}$  was most reliably initiated at 100 ms, suggesting a  $\text{Ca}^{2+}$  window or limit exists for triggering  $I_{\text{PD}}$ . Consistent with this, modestly broader action potentials, evoked by lengthening the train current-pulse duration, resulted in smaller prolonged depolarizations. With respect to the properties of  $I_{\text{PD}}$ , it displayed a linear current–voltage relationship with a reversal potential of about  $-45$  mV that was shifted to approximately  $-25$  mV by lowering internal  $\text{K}^+$  or about  $-56$  mV by lowering external  $\text{Na}^+$  and  $\text{Ca}^{2+}$ .  $I_{\text{PD}}$  was blocked by  $\text{Gd}^{3+}$ , but was not antagonized by MDL-123302A, SKF-96365, 2-APB, tetrodotoxin, or flufenamic acid. Optimal  $\text{Ca}^{2+}$  influx may activate calmodulin kinase and a voltage-independent, nonselective cation channel to initiate the prolonged depolarization, thereby contributing to the afterdischarge and reproduction.

## INTRODUCTION

In many systems, neuronal excitability can be modulated in an activity-dependent manner. This manifests as an alteration in responsiveness, membrane potential, or activity after a transient barrage of synaptic inputs or action potentials (Zhang and Linden 2003). For example, such inputs can elicit relatively short, depolarizing afterpotentials that last milliseconds to seconds, or more lengthy depolarizations that endure for minutes, as well as plateau potentials that are the result of entering a state with bistable membrane potentials (Dembrow et al. 2004; Egorov et al. 2002; Eyzaguirre and Kuffler 1955; Haj-Dahmane and Andrade 1997; Hasuo et al. 1990; Russell and Hartline 1982; Tasaki et al. 1954; Thompson and Smith 1976; Zhang et al. 1995). Responses of this nature can sensitize a neuron to subsequent stimulation or even drive the cell to fire spontaneously. As such, they represent an essential means for information storage, initiating behavior, or responding to nox-

ious stimuli. Improper regulation of the ion channels that mediate these responses may lead to pathologies such as epilepsy (Fraser and MacVicar 1996).

Prolonged depolarizations and plateau potentials are quite often long-lived activity-dependent changes, outlasting the stimulus duration many times over (Andrew and Dudek 1983; Egorov et al. 2002; Morriset and Nagy 1999; Rekling and Feldman 1997). In certain instances, the stimulus promotes voltage-gated  $\text{Ca}^{2+}$  entry and depolarizes the cell through activation of a nonselective cation current (Bal and McCormick 1993; Derjean et al. 2005; Morriset and Nagy 1999; Rekling and Feldman 1997; Zhang et al. 1995). Alternatively, the voltage change that occurs during the stimulus can on its own recruit persistent  $\text{Na}^+$  or  $\text{Ca}^{2+}$  currents to directly depolarize neurons (Aracri et al. 2006; Lo and Erzurumlu 2002; Mercer et al. 2005; Russo and Hounsgaard 1996; Sierra et al. 2005). Some of these activity-dependent changes also require the presence of a permissive neuromodulator (Derjean et al. 2005; Fraser and MacVicar 1996; Li et al. 1999; Perrier and Hounsgaard 2003).

The bag cell neurons of the marine mollusc, *Aplysia californica*, have long been used to study fundamental mechanisms by which activity is translated into long-term intrinsic change. These neuroendocrine cells form two distinct clusters of 200–400 neurons at the base of the pleurovisceral connectives, just rostral to the abdominal ganglia (Blankenship and Haskins 1979; Kupfermann 1967; Kupfermann and Kandel 1970). On brief synaptic input, the bag cell neurons undergo a roughly 30-min afterdischarge, consisting of depolarization, spiking, and the release of egg-laying hormone (Chiu et al. 1979; Dudek et al. 1979; Kupfermann 1967, 1970; Pinsker and Dudek 1977; Stuart et al. 1980). Egg-laying hormone is directly linked to egg-laying behavior, principally through its action on other neurons and peripheral structures, such as the ovitestic (Brown and Mayeri 1989; Mayeri et al. 1979a,b; Rothman et al. 1983; Scheller et al. 1982; Sigvardt et al. 1986; Stuart and Strumwasser 1980).

Previously, Whim and Kaczmarek (1998) found that a 1-Hz, 20-s train of action potentials delivered to bag cell neurons induced what they termed a depolarizing afterpotential that lasted several minutes. Decreasing extracellular  $\text{Ca}^{2+}$  or buffering intracellular  $\text{Ca}^{2+}$  with BAPTA-AM abolished the response, suggesting a dependency on  $\text{Ca}^{2+}$  influx. The present study examines the nature of the  $\text{Ca}^{2+}$  dependency of this response, which we designate a *prolonged depolarization*, and finds that there is a preferred level of  $\text{Ca}^{2+}$  influx for its

Address for reprint requests and other correspondence: N. S. Magoski, Department of Physiology, Queen's University, 4th Floor, Botterell Hall, 18 Stuart Street, Kingston, ON, K7L 3N6, Canada (E-mail: magoski@post.queensu.ca).

The costs of publication of this article were defrayed in part by the payment of page charges. The article must therefore be hereby marked "advertisement" in accordance with 18 U.S.C. Section 1734 solely to indicate this fact.

initiation. Furthermore, the depolarization depends on the recruitment of calmodulin kinase and the subsequent activation of a voltage-independent, nonselective cation channel. In vivo, this prolonged depolarization may provide drive for the after-discharge and thus contribute to species propagation. In general, such activity-dependent changes in membrane potential allow the nervous system to translate short-term commands into long-term behavioral events.

## METHODS

### *Animals and cell culture*

Adult *Aplysia californica* weighing 150–500 g were obtained from Marinus (Long Beach, CA). Animals were housed in an approximate 300-L aquarium containing continuously circulating, aerated seawater (Instant Ocean; Aquarium Systems, Mentor, OH, or Kent Marine, Acworth, GA) at 14–16°C on a 12/12-h light/dark cycle and fed romaine lettuce three to five times a week.

For primary cultures of isolated bag cell neurons, animals were anesthetized by an injection of isotonic  $MgCl_2$  (roughly 50% body weight); the abdominal ganglion was removed and incubated for 18 h at 22°C in neutral protease (13.33 mg/ml, 165859; Roche Diagnostics, Indianapolis, IN) dissolved in tissue culture artificial seawater (tcASW) [composition in mM: 460 NaCl, 10.4 KCl, 11  $CaCl_2$ , 55  $MgCl_2$ , 15 *N*-2-hydroxyethylpiperazine-*N'*-2-ethanesulfonic acid (HEPES), 1 mg/ml glucose, 100 U/ml penicillin, and 0.1 mg/ml streptomycin, pH 7.8 with NaOH]. The ganglion was then transferred to fresh tcASW and the bag cell neuron clusters were dissected from the surrounding connective tissue. Using a fire-polished Pasteur pipette and gentle trituration, neurons were dispersed onto 35 × 10-mm polystyrene tissue culture dishes (430165; Corning, Corning, NY) filled with 2 ml tcASW. Cultures were maintained in tcASW for 1–3 days in a 14°C incubator. Experiments were performed on neurons that were in vitro for ≥1 day. Salts were obtained from Fisher Scientific (Ottawa, ON, Canada) or Sigma (St. Louis, MO).

### *Sharp-electrode current-clamp recordings*

Current-clamp recordings were made from bag cell neurons using an AxoClamp 2B (Axon Instruments, Union City, CA) amplifier and the sharp-electrode, bridge-balanced method. Microelectrodes were pulled from borosilicate glass capillaries (1.2-mm ID, TW120F-4; World Precision Instruments, Sarasota, FL) and had a resistance of 5–20 MΩ when filled with 2 M K-acetate plus 10 mM HEPES and 100 mM KCl (pH = 7.3 with KOH). Current was delivered with either Clampex software (version 8.2; Axon Instruments) or a S88 stimulator (Grass, Warwick, MA). Voltage was filtered at 3 kHz using the Axoclamp built-in Bessel filter and sampled at 2 kHz using a Digidata 1322A A/D converter (Axon Instruments), an IBM-compatible personal computer, and Clampex. Current clamp was performed in normal artificial sea water (nASW; composition according to tcASW but lacking glucose, penicillin, and streptomycin). To broaden action potentials, tetraethylammonium (TEA, 20 or 50 mM; Acros Organics, Morris Plains, NJ) was added to nASW. With the exception of action potential amplitude and width, all voltage traces were filtered off-line to 20 Hz using Clampfit (version 8.2; Axon Instruments) for display. The very slow nature of the prolonged depolarization ensured that no change in amplitude or kinetics was brought about by this second filtering.

To test for neuronal input resistance, five sequential current steps were given, starting with a step of –50 pA and each step thereafter increasing by +25 pA. Using Ohm's law and the steady-state voltage change of the most stable step (typically, this was the first step to –50 pA), the resistance of the cell was determined.

### *Whole cell voltage-clamp recordings*

Voltage-clamp recordings were made using an EPC-8 amplifier (HEKA Electronics; Mahone Bay, NS, Canada) and the tight-seal, whole cell method. Microelectrodes were pulled from borosilicate glass capillaries (1.5-mm ID, TW150F-4; World Precision Instruments) and had a resistance of 1–2 MΩ when filled with various intracellular salines. Pipette junction potentials were nulled immediately before seal formation. Pipette and neuronal capacitive currents were canceled and, after breakthrough, the series resistance (3–5 MΩ) was compensated to 80% and monitored throughout the experiment. Cell capacitance was derived from the EPC-8 whole cell capacitance compensation. Current was filtered at 1 kHz with the EPC-8 built-in Bessel filter and sampled at 2 kHz according to the voltage (see above). Most recordings were made with nASW externally and regular intracellular saline internally [composition (in mM): 500 K-aspartate, 70 KCl, 1.25  $MgCl_2$ , 10 HEPES, 11 glucose, 10 glutathione, 5 ATP (grade 2, disodium salt; Sigma), and 0.1 GTP (type 3, disodium salt; Sigma); pH 7.3 with KOH]. For experiments where intracellular  $Ca^{2+}$  was weakly buffered, the regular intracellular saline contained added 0.1 mM EGTA. The free  $Ca^{2+}$  concentration of this saline was set at 300 nM by adding the appropriate amount of  $CaCl_2$ , as calculated by WebMaxC (<http://www.stanford.edu/~cpatton/webmaxcS.htm>) (courtesy of Dr. C. Patton, Stanford University, Palo Alto, CA). A junction potential of 15 mV was calculated for both of the above intracellular salines and compensated for by subtraction off-line. According to the voltage recordings, current traces were filtered after acquisition to 20 Hz for presentation using Clampfit.

Experiments designed to examine the reversal potential of the prolonged depolarization current ( $I_{PD}$ ) required external,  $Na^+$  and  $Ca^{2+}$ , or internal  $K^+$  substitutions. The two external solutions used were 1) low  $Na^+$  ASW [composition (in mM): 460 NMDG, 10.4 KCl, 55  $MgCl_2$ , 11  $CaCl_2$ , 15 HEPES; pH 7.8 with NaOH], and 2) low  $Na^+/Ca^{2+}$  ASW [composition (in mM): 471 NMDG, 10.4 KCl, 66  $MgCl_2$ , 15 HEPES; pH 7.8 with KOH]. These salines were designated as “low” because of contamination from other salts; as such, we estimate that there is about 2.4 mM  $Na^+$  in the low  $Na^+$  saline, whereas the low  $Na^+/Ca^{2+}$  contains about 2.5 mM  $Na^+$  and about 0.65 mM  $Ca^{2+}$ . Internally, much of the  $K^+$  was replaced with a low  $K^+$  saline [composition (in mM): 70 KCl, 10 HEPES, 11 glucose, 10 glutathione, 500 aspartic acid, 500 NMDG, 5 ATP, and 0.1 GTP; pH 7.3 with KOH]. Junction potentials of 23 mV for either the low  $Na^+$  or low  $Na^+/Ca^{2+}$  ASW versus the regular intracellular saline and 9 mV for low  $K^+$  intracellular versus nASW were compensated for by subtraction off-line.

$Ca^{2+}$  currents were isolated using an ASW where the  $Na^+$  was replaced with TEA and the  $K^+$  with  $Cs^+$  [composition (in mM): 460 TEA-Cl, 10.4 CsCl, 55  $MgCl_2$ , 11  $CaCl_2$ , 15 HEPES; pH 7.8 with CsOH]. Also, the protocol used an intracellular saline where the  $K^+$  was replaced with  $Cs^+$  [composition (in mM): 70 CsCl, 10 HEPES, 11 glucose, 10 glutathione, 5 EGTA, 500 aspartic acid, 5 ATP, and 0.1 GTP; pH 7.3 with CsOH]. On-line leak subtraction was performed in some instances using a *P/4* protocol from –60 mV with subpulses of opposite polarity and one fourth the magnitude, an intersubpulse interval of 500 ms, and 100 ms before actual test pulses. A junction potential of 20 mV was compensated for by subtraction off-line.

### *Reagents and drug application*

Most drugs were applied using a gravity-driven perfusion system before giving any stimulus. The exceptions to this were  $Gd^{3+}$ , MDL-123302A, SKF-96365, and 2-APB, which were perfused immediately after the stimulus, as well as tetrodotoxin (TTX), which was added manually to the dish, before the stimulus. Drugs that used distilled water as the vehicle included: 2-aminoethoxydiphenylborate (2-APB, 100065; Calbiochem, San Diego, CA),  $GdCl_3$  (G-7532;

Sigma), *cis-N*-(2-phenylcyclopentyl)-azacyclotridec-1-en-2-amine hydrochloride (MDL-123302A; M-182; Sigma), 1-[ $\beta$ -[3-(4-methoxyphenyl)propoxy]-4-methoxyphenethyl]-1H-imidazole hydrochloride (SKF-96365, 567310; Calbiochem), and tetraethylammonium (TEA, AC150905000; Fisher). Sodium citrate tribasic dehydrate (S4641; Sigma) in water was used as the vehicle for TTX (T-550; Alomone Labs, Jerusalem, Israel); ethanol was used for *N*-(3-[trifluoromethyl]phenyl)anthranilic [flufenamic acid (FFA), F-9005; Sigma]; and dimethyl sulfoxide (DMSO, BP231-1; Fisher) was used for KN-62 (I-2142; Sigma). KN-62 stock was mixed with 500  $\mu$ l of nASW and this solution exchanged for an equal amount of nASW from the culture dish. Dishes were incubated for 10–15 min before experimentation. Ni<sup>2+</sup> block of Ca<sup>2+</sup> currents was achieved by dissolving appropriate amounts of NiCl<sub>2</sub> (N6136; Sigma) in nASW for final concentrations ranging from 300  $\mu$ M to 10 mM. Calmodulin binding domain (CBD), corresponding to residues 290–309 of rat brain calmodulin kinase II regulatory domain (Payne et al. 1988) (208734; Calbiochem), was dissolved in regular intracellular saline plus 1% Fast Green (BP123-10; Fisher). CBD was pressure injected into neurons by sharp electrode with 300-ms pulses at 5–10 psi using a PMI-100 pressure microinjector (Dagan, Minneapolis, MN) and experiments were performed about 4 min after injection. The vehicle for CBD was water. Other calmodulin kinase antagonists tested included calmidazolium chloride (208665; Calbiochem), chlorpromazine hydrochloride (C8138; Sigma), and trifluoperazine dihydrochloride (T8516; Sigma). These drugs were added as stock solutions directly into dishes of cultured neurons and incubated for 10–15 min before experimentation.

### Analysis

Clampfit was used to determine peak amplitude of either the prolonged depolarization or the prolonged depolarization current ( $I_{PD}$ ). Cursors were placed at the baseline voltage or current, before delivery of the stimulus, as well as at peak voltage or current amplitude after the stimulus. The difference between the two cursor values was taken as the amplitude. Action potential amplitude and half-widths were determined using Clampfit and by setting cursors at the start and end of the action potential. The current–voltage relationship of the Ca<sup>2+</sup> current was determined by measuring peak current

between cursors set at the start and end of the traces in Clampfit. Current was normalized to cell size by dividing by the whole cell capacitance and plotted against voltage. To calculate total divalent ionic influx of Ca<sup>2+</sup>, the area above each current trace was calculated in Clampfit, summed in Origin (version 7.0; OriginLab, Northampton, MA), and divided by whole cell capacitance.

Reversal potentials were determined by taking the difference current from a voltage ramp given before delivery of the stimulus train (see RESULTS) from a ramp given after. Conductance was derived using modified Ohm's law and the current during a 200-ms step from –60 to –70 mV. The percentage change was calculated from the conductance before and after stimulus delivery.

Hill curve fits were generated in Origin and provided the 50% inhibitory concentration (IC<sub>50</sub>; the concentration of the antagonist that is required for 50% inhibition) as well as the Hill coefficient (a coefficient >1 denotes positive binding cooperativity between the ligand and receptor).

Data are presented as means  $\pm$  SE as calculated using either Origin or InStat (version 3.05; GraphPad Software; San Diego, CA). Statistical analysis was performed using InStat. A one-sample *t*-test was used to determine whether the mean of a single group was different from a mean of zero. Student's *t*-test was used to test whether the mean differed between two groups. Comparisons between three or more means used a one-way ANOVA and a Bonferroni multiple-comparisons post hoc test or a test for linear trend. Unless otherwise stated, all tests are two-tailed. Data were considered significantly different if the *P* value was <0.05.

## RESULTS

### A prolonged depolarization in cultured bag cell neurons

Under sharp-electrode current clamp at –60 mV, action potentials evoked at 5 Hz for 10 s by current injection elicited a lengthy depolarization of about 10 mV ( $n = 76$ ) from cultured bag cell neurons with a mean input resistance of about 390 M $\Omega$  ( $n = 59$ ) (Fig. 1, *A* and *C*). Action potential broadening was detected throughout the train (Fig. 1*B*). Although the depolarization lasted for extended periods of time, most traces were terminated 4–5 min after stimulus delivery, once a

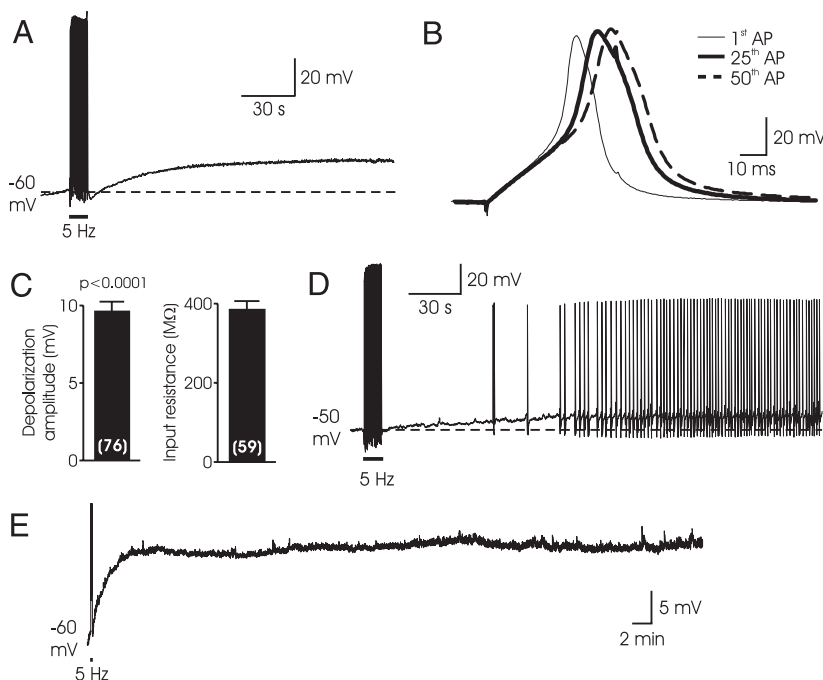


FIG. 1. A prolonged depolarization in cultured bag cell neurons. *A*: example of a nearly 15-mV prolonged depolarization generated by a train of 50-ms square current pulses at 5 Hz, 10 s in normal artificial seawater (nASW) under sharp electrode, current clamp at –60 mV. Burst of action potentials (APs) from the stimulus appears as a thick vertical bar resulting from the condensed time base. In *A*, *C*, and *D*, the membrane potential is recorded for about 4 min. Depolarization remains elevated until termination of the recording. *B*: example of APs generated during the stimulus in *A*. Although AP amplitude does not change appreciably, width increases during the train. *C*: graphs of the average prolonged depolarization amplitude and the average input resistance. Change in membrane potential during the prolonged depolarization is significantly different from zero (one-sample *t*-test). For this and subsequent bar graphs, the number of experiments is indicated in brackets either above, within, or below the bars. *D*: example of a stimulus that generated a depolarization that resulted in persistent, spontaneous spiking (representative of  $n = 6$ ; not included in *C*). Average frequency of spiking for this neuron is 0.5 Hz. *E*: some prolonged depolarizations show long duration. This neuron is held at –60 mV and given the standard stimulus of 50-ms square current pulses at 5 Hz for 10 s in nASW, producing a response that remains elevated for >30 min. Note that the scale bars are different between *A* and *D*. APs are truncated at the top.

plateau had been reached. On occasion, the depolarization led to spontaneous action potentials, lasting >8 min with an average frequency of 0.3 Hz ( $n = 6$ ) (Fig. 1D). The neuron displayed in Fig. 1D was current clamped at  $-50$  mV because it was involved in preliminary studies where neurons were held at various voltages ( $-60$ ,  $-50$ , or  $-40$  mV) to find an optimal membrane potential from which the prolonged depolarization could be induced. The optimal holding voltage was  $-60$  mV and is used throughout. A standard current train of 50-ms pulses at 5 Hz, 10 s consistently elicited prolonged depolarizations compared with other frequencies (data not shown). Some depolarizations, without spontaneous action potentials, were observed to last for >30 min ( $n = 3$ ) (Fig. 1E). Whim and Kaczmarek (1998) termed a similar response in bag cell neurons a depolarizing afterpotential; however, given the lengthy duration of the response that is the subject of the present study, we have designated it a *prolonged depolarization*.

#### The prolonged depolarization involves calmodulin kinase

The previous description of the response showed a strong dependency on action potential broadening and  $\text{Ca}^{2+}$  influx during the stimulus (Whim and Kaczmarek 1998). Thus a role for calmodulin kinase, a protein commonly activated by  $\text{Ca}^{2+}$  influx (DeReimer et al. 1984; Hanson and Schulman 1992; Xu et al. 2005), was examined. Calmodulin kinase II antagonists, KN-62 (Tokumitsu et al. 1990) and calmodulin binding domain (CBD) (Payne et al. 1988) were tested under sharp-electrode current clamp. Neurons were given a standard current train from  $-60$  mV to elicit the prolonged depolarization. At a concentration of  $10 \mu\text{M}$ , KN-62 significantly attenuated depolarization amplitude compared with DMSO (the vehicle) (Fig. 2A) ( $n = 7$  and  $n = 6$ ). In eight of nine neurons injected with CBD, the depolarization was reduced compared with those injected with water (the vehicle) ( $n = 13$ ) (Fig. 2B). This resulted in a CBD data set that was significantly different from control.

Other calmodulin kinase antagonists proved difficult to use. Application of 1 or  $10 \mu\text{M}$  calmidazolium,  $100 \mu\text{M}$  trifluoperazine, or  $100 \mu\text{M}$  chlorpromazine, using the same protocol as KN-62, induced detachment and death during or shortly after the 10- to 15-min incubation period. Therefore no experiments could be completed in the presence of these drugs. Between five and ten dishes were used for each of these experiments.

#### Action potential broadening and the effect of TEA on prolonged depolarization amplitude

Because  $\text{Ca}^{2+}$  influx is crucial for generating the prolonged depolarization (Whim and Kaczmarek 1998), we examined whether increasing action potential width and  $\text{Ca}^{2+}$  influx would influence its amplitude. TEA was used to block  $\text{K}^{+}$  channels (Hagiwara and Saito 1959) and broaden action potentials during the stimulus train (Klein and Kandel 1978; Quattrocci et al. 1994). Surprisingly, the depolarization amplitude decreased, in a concentration-dependent fashion, after 20 and 50 mM TEA ( $n = 5$  and 5) compared with control ( $n = 18$ ) (Fig. 3). As depicted in Fig. 4A, application of 20 and 50 mM TEA significantly and appreciably broadened action potential width compared with that of control. Only control action potentials broadened significantly throughout the train. Because action potentials were wider in TEA at all times, including at the start of the train, they did not broaden further during the train (Fig. 4B, right). Half-way through the train, action potential amplitude was the same in all conditions (about 90 mV) (Fig. 4B, left). TEA would have consistently resulted in larger  $\text{Ca}^{2+}$  influx, suggesting that greater  $\text{Ca}^{2+}$  influx does not incur larger prolonged depolarizations, but rather decreases the amplitude.

#### The prolonged depolarization current ( $I_{PD}$ )

The results thus far show that increasing action potential width with TEA does not potentiate the prolonged depolarization, and yet  $\text{Ca}^{2+}$  and calmodulin kinase are involved in the mechanism. Considering this, there may be a specific window of  $\text{Ca}^{2+}$  influx or a limitation as to how much  $\text{Ca}^{2+}$  influx is required to generate  $I_{PD}$ . To accurately control voltage and  $\text{Ca}^{2+}$  influx while eliciting  $I_{PD}$ , whole cell voltage clamp was carried out. With nASW externally and regular intracellular saline in the pipette (K-aspartate based, no  $\text{Ca}^{2+}$  buffer),  $I_{PD}$  was induced from  $-60$  mV using square pulses, in lieu of action potentials, to  $+10$  mV (the peak of the  $\text{Ca}^{2+}$  current; see following text). Pulse duration was varied (10, 25, 50, 75, 100, 150 ms) and intracellular  $\text{Ca}^{2+}$  buffered (no buffer vs. 0.1 mM EGTA) to find an optimal condition for reliably eliciting  $I_{PD}$ . Pulse durations >150 ms were not attempted because this approaches the 5-Hz limit and would result in poor voltage clamp.

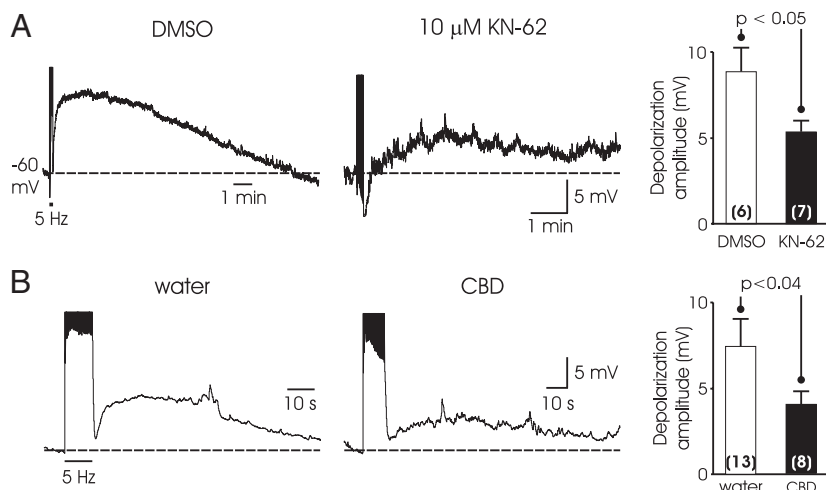


FIG. 2. Calmodulin kinase may be involved in prolonged depolarization generation. *A, left*: sample traces denoting the effects of 0.06% dimethyl sulfoxide (DMSO, the vehicle) or  $10 \mu\text{M}$  KN-62, a calmodulin kinase antagonist, on the prolonged depolarization under current clamp at  $-60$  mV. Neurons are incubated with DMSO or KN-62 for 10–15 min before experimentation. *Right*: summary graph showing that KN-62 significantly attenuates the depolarization amplitude (unpaired  $t$ -test). *B, left*: traces depicting the effects after injection of water (the vehicle) or calmodulin binding domain (CBD, 1 mM in electrode) on prolonged depolarization amplitude. There is a minimum postinjection incubation period of 4 min before experimentation. *Right*: summary graph showing that CBD injection significantly reduces the depolarization amplitude compared with that of water (unpaired, one-tailed  $t$ -test).

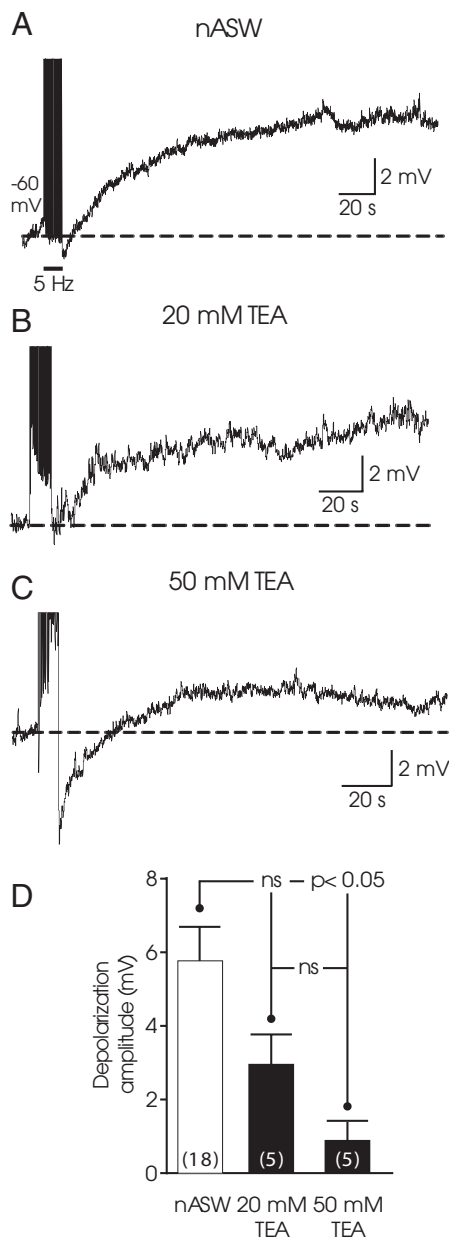


FIG. 3. Tetraethylammonium (TEA) reduces prolonged depolarization amplitude. *A–C*: examples of prolonged depolarizations generated in 3 separate neurons current clamped at  $-60$  mV. Each neuron is bathed in nASW, 20 or 50 mM TEA before delivering the standard current stimulus. As the concentration of TEA increases, the depolarization decreases. *D*: summary graph showing that neurons perfused with TEA exhibit lower prolonged depolarization amplitudes. Comparing the depolarization amplitude in nASW vs. TEA, there is a significant difference only between control and 50 mM TEA (ANOVA, Bonferroni's multiple-comparisons test), but a test for linear trend between all 3 conditions is significant ( $P < 0.02$ ).

After a voltage stimulus train, there was a slow, inward current that typically peaked within 20–30 s, usually lasted 3–5 min, and was sometimes preceded by a rapid outward current (Fig. 5*A*). None of the pulse durations significantly affected the amplitude of peak  $I_{PD}$  (Fig. 5*B*, left). However, the frequency of  $I_{PD}$  occurrence was sensitive to pulse duration, i.e., the number of instances where a bona fide  $I_{PD}$  could be documented varied with the length of the voltage pulse delivered during the train. The criterion for identifying an  $I_{PD}$  was if the

inward current after the train was  $-1$  pA or greater when compared with the current before the train. With regular intracellular saline, the optimal pulse duration for  $I_{PD}$  occurrence was 100 ms (93%) (Fig. 5*B*, right). Increasing the pulse duration to 150 ms lowered the frequency of  $I_{PD}$  to 75%. Decreasing the pulse duration to  $<100$  ms also resulted in a lowered  $I_{PD}$  occurrence, but the response was not eliminated entirely. Expectedly, intracellular saline containing 0.1 mM of the slow  $Ca^{2+}$  buffer EGTA (Naraghi and Neher 1997) decreased  $I_{PD}$  occurrence for all but one of the six pulse durations (Fig. 5*C*, right). Again, occurrence of the response was not completely eliminated in the presence of EGTA, although because the frequency was reduced, the absolute number of responses used to calculate average  $I_{PD}$  amplitude was low (Fig. 5*C*, left). Whim and Kaczmarek (1998) found that the fast  $Ca^{2+}$  buffer BAPTA-AM (Naraghi and Neher 1997) also decreased the amplitude of the response. Subsequently, to elicit  $I_{PD}$ , neurons were given a standard voltage stimulus of 100-ms pulses from  $-60$  to  $+10$  mV at 5 Hz for 10 s with regular intracellular saline in the whole cell pipette.

We have interpreted the ability of TEA to decrease the prolonged depolarization amplitude as arising from an excess of  $Ca^{2+}$  influx. However, there is the possibility that this inhibition results from TEA having a nonspecific effect on  $I_{PD}$ . To test this, 50 mM TEA was applied under voltage clamp, using regular intracellular saline in the pipette, and the standard voltage stimulus was delivered to evoke  $I_{PD}$ . Compared with nASW alone, TEA did not alter  $I_{PD}$  ( $-68.3 \pm 17.8$  vs.  $-48.8 \pm 9.9$  pA;  $n = 6$  and  $n = 5$ ; unpaired  $t$ -test, not significant), suggesting that inhibition of the prolonged depolarization by TEA was the result of increasing action potential duration and  $Ca^{2+}$  influx, rather than block of  $I_{PD}$  itself.

#### $Ca^{2+}$ current during the voltage stimulus

Both the EGTA data and the results from the study by Whim and Kaczmarek (1998) suggest that voltage-gated  $Ca^{2+}$  influx is important for generating the depolarization. To examine  $Ca^{2+}$  influx more closely,  $Ca^{2+}$  current was isolated by whole cell voltage clamp, with  $Cs^{+}$  replacing  $K^{+}$  in the internal saline and  $Cs^{+}$  and TEA replacing  $K^{+}$  and  $Na^{+}$ , respectively, in the external ASW. Initially, bag cell neurons were voltage clamped at  $-60$  mV and given 200-ms steps from  $-60$  to  $+60$  mV in 10-mV increments. During the pulses,  $Ca^{2+}$  current was relatively fast activating, strongly voltage dependent, moderately inactivating, and maximal at  $+10$  mV (Fig. 6, *A* and *B*).

We next compared the level of  $Ca^{2+}$  influx during the stimulus train at the various pulse durations used to elicit  $I_{PD}$ . Up to this point, the leak and capacitive currents were subtracted from  $Ca^{2+}$  currents with the  $P/4$  protocol (see METHODS), but because of the inordinate amount of time required for  $P/4$  during a train, post- $Ni^{2+}$ -block subtraction was used. Figure 6*C* shows the concentration-inhibition curve of  $Ni^{2+}$  for  $Ca^{2+}$  current, where full block occurs at 10 mM. Thus 10 mM  $Ni^{2+}$  was used to block  $Ca^{2+}$  currents and the remaining current was then subtracted from previous  $Ca^{2+}$  traces. Neurons were held at  $-60$  mV and given square voltage steps of 10, 25, 50, 75, 100, or 150 ms from  $-60$  to  $+10$  mV at 5 Hz for 10 s. At pulse durations of 10 or 25 ms, the  $Ca^{2+}$  current showed little use-dependent inactivation, but for 50–150 ms, the current declined steadily after the first few steps (Fig. 6*D*).

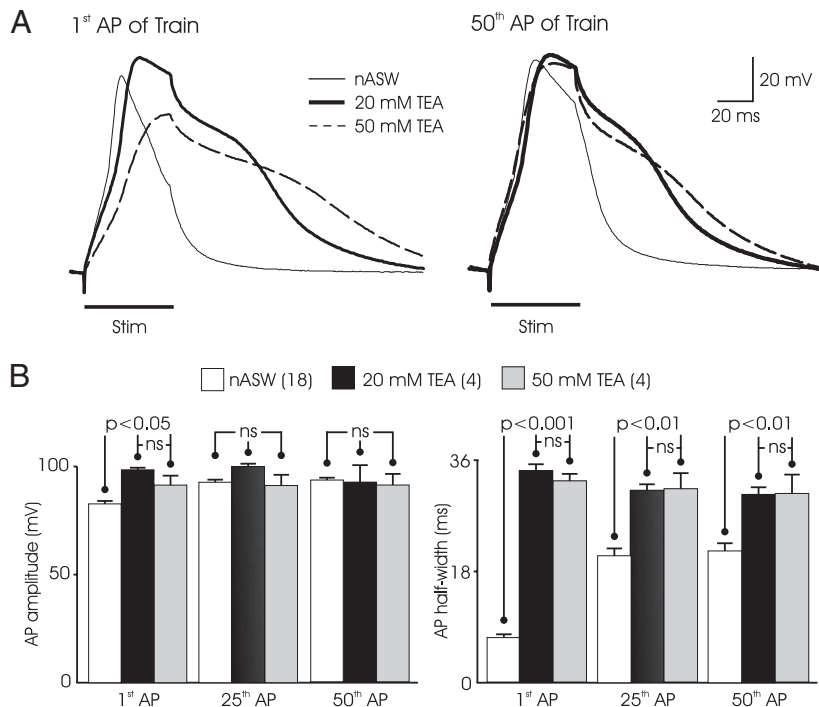


FIG. 4. TEA induces action potential broadening. *A*: sample APs from the start and end of a standard current train in nASW, 20 or 50 mM TEA. APs become increasingly broad as the concentration of TEA increases. Neurons perfused with TEA show far broader APs to begin with; however, only nASW APs show obvious broadening between the start and the end of the train. *B*: summary graphs comparing AP amplitude and half-width between the 1st, 25th, and 50th APs in nASW, 20 and 50 mM TEA. *Left*: only the amplitude of the 1st AP is significantly different between nASW and TEA and there is no difference between the two TEA concentrations (ANOVA, Bonferroni's multiple-comparisons test). *Right*: TEA application results in a significant difference compared with control for all AP half-widths (ANOVA, Bonferroni's multiple-comparisons test), but there is no difference between the two concentrations of TEA.

$\text{Ca}^{2+}$  influx was measured by summing the area above the  $\text{Ca}^{2+}$  current from each individual trace during the train and normalizing it to cell capacitance. Despite the greater use-dependent inactivation,  $\text{Ca}^{2+}$  influx increased linearly with pulse duration (Fig. 6E). Nevertheless, although  $\text{Ca}^{2+}$  current continued to rise, optimal  $I_{\text{PD}}$  frequency was detected at 100 ms (see Fig. 5B, right).

#### Current-pulse duration alters action potential half-width and prolonged depolarization amplitude

Although the results are consistent with a  $\text{Ca}^{2+}$  window or limit for generating the prolonged depolarization, it is unexpected that  $I_{\text{PD}}$  frequency, but not amplitude, decreased with longer voltage pulses. It is possible that the whole cell recording conditions (i.e., washout) contributed to this phenomenon. Thus we again used sharp-electrode current clamp and attempted to better titrate action potential half-width, using different current-pulse durations instead of TEA, when triggering the prolonged depolarization. Current trains of 5 Hz, 10 s were delivered from  $-60$  mV in nASW using pulse durations of 10, 50, or 100 ms. Regardless of pulse duration, there was no difference in the half-width of the first action potential, although by the middle of the train, the action potentials evoked by the 100-ms pulses ( $n = 8$ ) were about 10 ms longer than those evoked by the 10- and 50-ms pulses ( $n = 7$  and  $n = 7$ ) (Fig. 7, A and B). Although significant, this broadening was not as large as that seen with TEA. There was also a clear and statistically significant linear trend for a decrease in the size of the prolonged depolarization as the current-pulse duration of the stimulus train was increased (Fig. 7C). The average depolarization elicited by 100-ms pulses was 45% smaller when compared with that elicited by 10-ms pulses, a decrease that reached the level of significance (Fig. 7D). However, there was no difference between the prolonged depolarization evoked by 10- versus 50-ms pulses or 50- versus 100-ms pulses (Fig. 7D).

Thus current pulses of a minimal duration produced normally broadened action potentials and presumably a smaller  $\text{Ca}^{2+}$  influx, resulting in an enhanced depolarization. Lengthy current pulses increased action potential duration, which suppressed the magnitude of the depolarization.

#### $I_{\text{PD}}$ reversal potential and ion substitution

$I_{\text{PD}}$  was further characterized by manipulating external and internal solutions under voltage clamp. The reversal potential and membrane conductance were determined at peak  $I_{\text{PD}}$  by delivering both a 200-ms step from  $-60$  to  $-70$  mV and a 5-s ramp from  $-80$  to  $+20$  mV, before and after the standard current stimulus train (Fig. 8A). The change in membrane conductance was calculated as a percentage change in current produced by the step given before versus the step given after the train. Reversal potential was derived from the ramp difference current, i.e., the current evoked by the ramp before the train subtracted from current evoked by the ramp after the train. There was an roughly 40% increase in conductance after the train ( $n = 43$ ) (Fig. 8B), suggesting that channel opening generates the prolonged depolarization. This is consistent with the findings of Whim and Kaczmarek (1998), who also observed an inward current with an increased steady-state conductance after a burst of action potentials in bag cell neurons. However, they did not further examine the nature of this current. When we determined the difference current elicited during the ramp, it was linear and showed no obvious voltage dependency (Fig. 8C). The difference current reversal potential under control conditions was about  $-45$  mV ( $n = 29$ ) (Fig. 8D), which is characteristic of a nonselective cation channel (Chakfe and Bourque 2000; Kramer and Zucker 1985; Partridge and Swandulla 1988). Lowering intracellular  $\text{K}^+$  levels from 570 to 70 mM shifted the reversal potential to  $-25$  mV ( $n = 7$ ), but replacing most external  $\text{Na}^+$  (from 460 to about

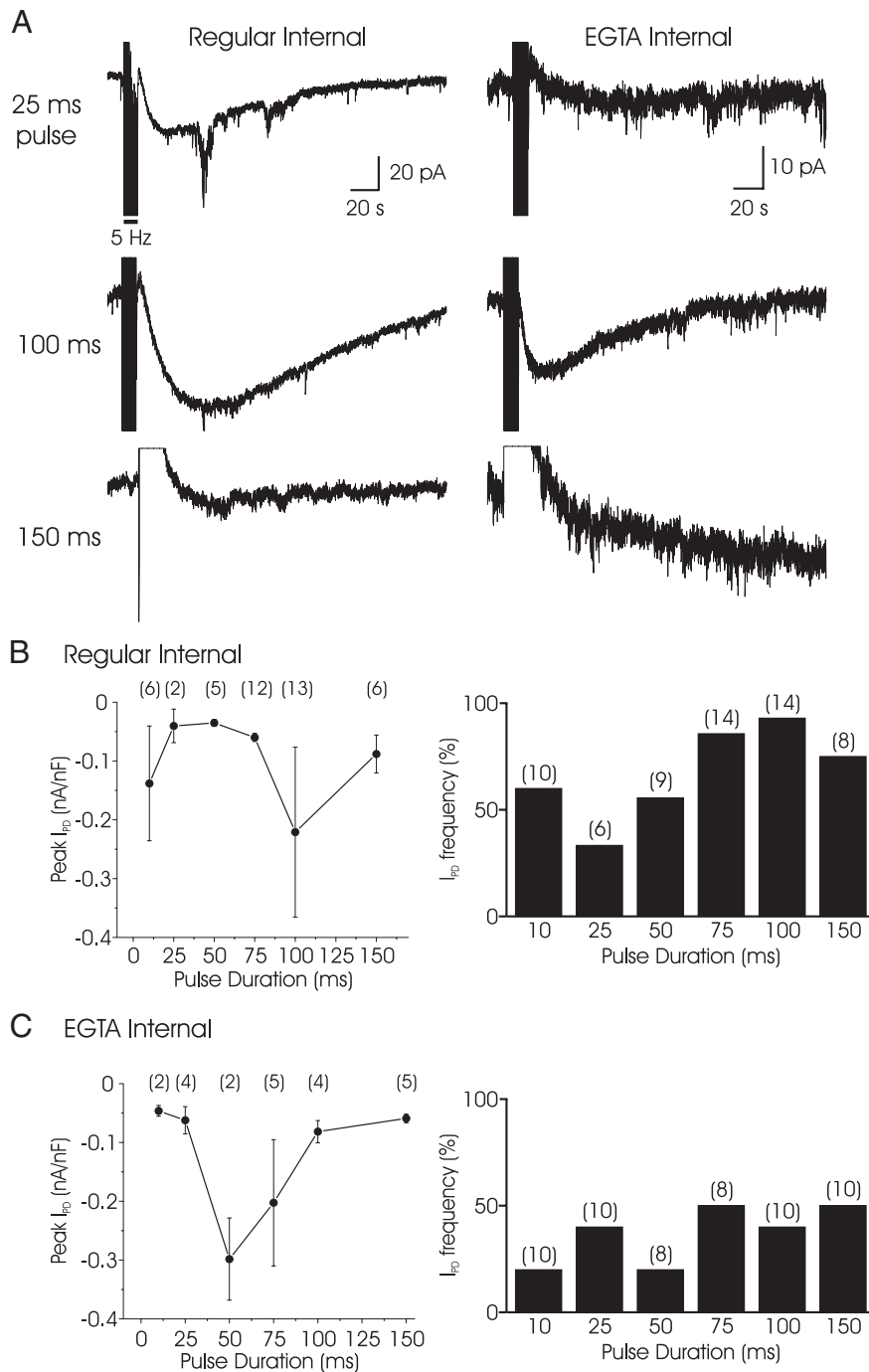


FIG. 5. Effect of pulse duration and intracellular  $Ca^{2+}$  buffering on prolonged depolarization current ( $I_{PD}$ ). *A*: whole cell, voltage-clamp traces of  $I_{PD}$  elicited after delivery of 25-, 100-, or 150-ms square pulses from  $-60$  to  $+10$  mV at 5 Hz for 10 s in nASW. *Left column*: regular intracellular saline (no added  $Ca^{2+}$ , no EGTA). *Right column*: EGTA internal solution (300 nM  $Ca^{2+}$ , 0.1 mM EGTA). Stimulus produces a "burst" of inward and outward currents that, as a result of the condensed time base, appear as a thick vertical bar. Current burst is truncated at the *top* and *bottom*. *B, left*: graph of the peak  $I_{PD}$  normalized to cell capacitance evoked by pulse durations ranging from 10 to 150 ms with regular intracellular saline. Because of the large SE throughout, the peak amplitudes are not significantly different. *n*-value for each data point includes only neurons that display an  $I_{PD}$ . *Right*: bar graph depicts the  $I_{PD}$  frequency of occurrence in neurons given different pulse durations. Overall, as the pulse duration increases, so does the occurrence of  $I_{PD}$ , until 100 ms, after which the frequency falls. *n*-value for each bar includes all neurons, i.e., those that display an  $I_{PD}$  (*right*) and those that do not. *C, left*: graph of normalized peak  $I_{PD}$  evoked by trains with various pulse durations with 0.1 mM EGTA  $Ca^{2+}$  buffering in the internal saline. Again, the amplitudes were not significantly different. *Right*: bar graph depicts  $I_{PD}$  frequency of occurrence in neurons at various pulse durations. Compared with regular intracellular saline, addition of EGTA into the internal solution decreases  $I_{PD}$  frequency in 5 of the 6 durations.

2.4 mM) with NMDG had no significant effect because the reversal potential stayed at about  $-44$  mV ( $n = 11$ ) (Fig. 8, *C* and *D*). However, the reversal potential did shift to approximately  $-56$  mV ( $n = 21$ ) after reducing both external  $Na^+$  from 460 to about 2.5 mM (with NMDG replacement) and  $Ca^{2+}$  from 11 to about 0.7 mM (with  $Mg^{2+}$  replacement) (Fig. 8, *C* and *D*). These results imply that a voltage-independent, nonselective cation channel, which conducts  $Na^+$ ,  $K^+$ , and perhaps  $Ca^{2+}$ , is involved in the prolonged depolarization. Because the  $Ca^{2+}$  levels of the low  $Na^+/Ca^{2+}$  ASW were insufficient to allow the train to trigger  $I_{PD}$  (data not shown), the current was first evoked in nASW and then the low  $Na^+/Ca^{2+}$  ASW was perfused onto neurons immediately after.

#### FFA does not block $I_{PD}$

Flufenamic acid (FFA) is one of the most widely used cation channel blockers (Ghamari-Langroudi and Bourque 2002; Haj-Dahmane and Andrade 1999; Morisset and Nagy 1999; Partridge and Valenzuela 2000). We assayed FFA on  $I_{PD}$ , but confounding side effects led to inconclusive results. Initially, 100 or 200  $\mu$ M FFA was tested, but neither concentration had an obvious effect on  $I_{PD}$  ( $n = 7$  and  $n = 4$ ) (data not shown). Often, high concentrations of FFA are required to block cation channels (e.g., Ghamari-Langroudi and Bourque 2002; Morisset and Nagy 1999; Partridge and Valenzuela 2000; Shaw et al. 1995). As such, we next used 300  $\mu$ M FFA, which generated

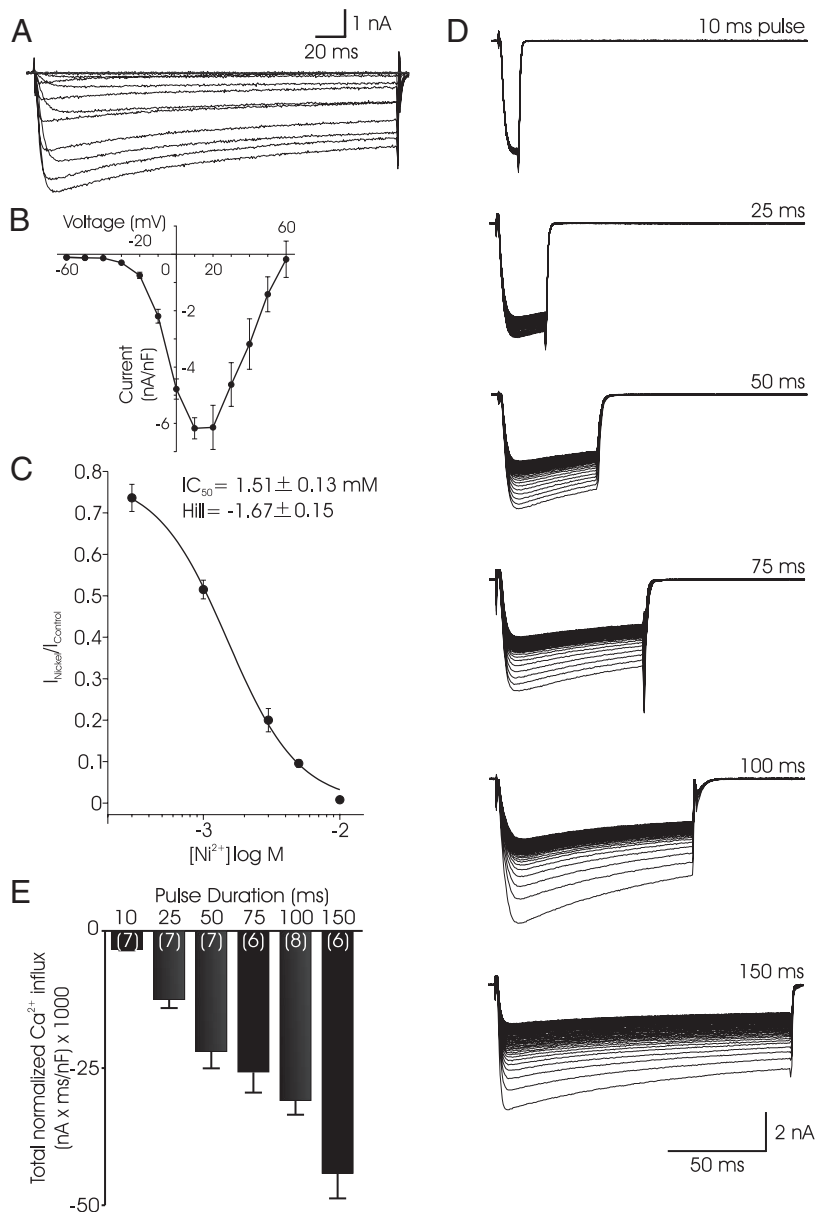


FIG. 6. Total Ca<sup>2+</sup> influx increases with increasing pulse duration. *A*, left: traces of Ca<sup>2+</sup> currents in neurons given 200-ms square pulses from -60 to +60 mV in 10-mV increments under voltage clamp at -60 mV. *B*: graph depicting current-voltage relationship for Ca<sup>2+</sup>. Peak current at each step is normalized to whole cell capacitance and averaged. Maximum inward current for Ca<sup>2+</sup> is at +10 mV. *C*: concentration-inhibition curve for Ni<sup>2+</sup> on Ca<sup>2+</sup> current. Neurons are voltage clamped at -60 mV and given one step to +10 mV. Different concentrations of Ni<sup>2+</sup> are perfused and the step is repeated. Current evoked in Ni<sup>2+</sup> is then divided by the control current and plotted against Ni<sup>2+</sup> concentration. IC<sub>50</sub> is about 1.5 mM, with a cooperative Hill coefficient approaching -2, and full block occurring at 10 mM. This concentration of Ni<sup>2+</sup> is used to isolate and subtract leak and other contaminating currents. *D*: superimposed traces of the Ca<sup>2+</sup> current elicited under voltage clamp at -60 mV during a 5-Hz, 10-s train of square pulses of 10–150 ms from -60 to +10 mV. *E*: summary graph showing total normalized Ca<sup>2+</sup> influx during the 5-Hz, 10-s train with pulse durations ranging from 10 to 150 ms. Total ionic influx is calculated by summing the area above each current pulse for a given duration and normalizing to cell capacitance. An ANOVA followed by a test for linear trend between the means shows a significant linear trend for greater influx with longer pulses ( $P < 0.0001$ ). Also, a Bonferroni multiple-comparisons test shows that total influx is significantly greater at 150 than at 100 ms ( $P < 0.02$ ).

a large outward current that gradually returned to baseline after about 30 min (Fig. 9A). Compared with control ( $n = 4$ ), 300  $\mu$ M FFA ( $n = 3$ ) considerably increased the holding current (Fig. 9B), suggesting possible secondary mechanisms. When the effects of FFA on holding current subsided, the standard voltage train was given and it generated an inward current ( $n = 5$ ) that was significantly greater than control ( $n = 6$ ) (Fig. 9, C and D). The current in the presence of FFA was also particularly unstable (see Fig. 9C).

*I*<sub>PD</sub> is blocked by the classic cation channel antagonist Gd<sup>3+</sup> but not by MDL-123302A, TTX, 2APB, or SKF-96365

To further test cation channel involvement in *I*<sub>PD</sub> generation, various cation channel blockers were used. TTX is classically known as a Na<sup>+</sup> channel blocker (Narahashi et al. 1964); however, at high concentrations it was shown to block a voltage-dependent cation channel in bag cell neurons (Wilson et al. 1996). Bag cell neurons were given two sequential stimuli

in the absence and presence of either 100  $\mu$ M TTX or citrate (the vehicle). To limit costs, TTX was not perfused, but added manually to the bath from a stock. As such, it was necessary to calculate the percentage change in peak *I*<sub>PD</sub> between the peak of the first and second *I*<sub>PD</sub>. This effectively measured current “rundown,” a phenomenon we noticed during initial testing, whereby additional stimuli after the initial train elicited progressively smaller *I*<sub>PD</sub>. Thus if citrate or TTX was effective in attenuating *I*<sub>PD</sub>, it would show a greater percentage decrease. The percentage change in *I*<sub>PD</sub> amplitude with citrate ( $-41.7 \pm 8.0\%$ ;  $n = 9$ ) or TTX ( $-44.5 \pm 6.2\%$ ;  $n = 9$ ) was not significantly different (unpaired *t*-test), implying the channel reported by Wilson et al. (1996) is not involved here. Note that Magoski et al. (2000) reported that 100  $\mu$ M TTX did not block bag cell neuron Ca<sup>2+</sup> currents; thus Ca<sup>2+</sup> influx is likely similar in both TTX and citrate.

Four agents found by others to block various cation channels, store-operated Ca<sup>2+</sup> channels, or transient receptor po-

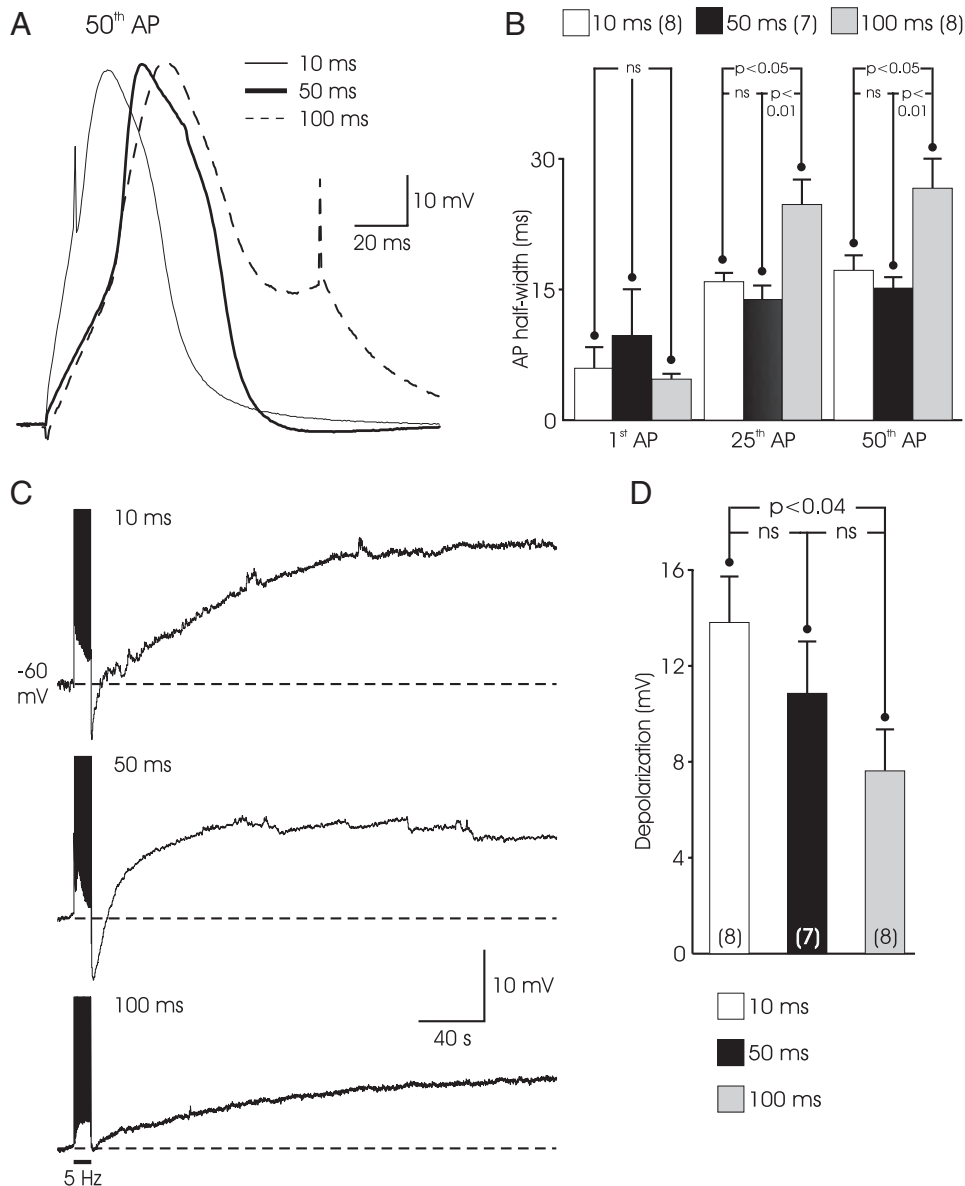


**FIG. 7.** Modest changes to AP duration alters the prolonged depolarization. *A*: sample APs in nASW from the end of a 5-Hz, 10-s current train with 10-, 50-, or 100-ms pulse duration. APs are of similar duration when evoked with 10- and 50-ms pulses, but are broader when triggered by a 100-ms pulse. Because of the large amount of current required simply to elicit an AP with the 10-ms pulses, it was often the case that they had a more rapid onset, particularly once the train was well under way. *B*: summary graph comparing half-width between the 1st, 25th, and 50th APs when evoked with 10-, 50-, or 100-ms current-pulse durations. Half-widths of the 1st AP show no difference between pulse durations. However, by the 25th and 50th APs, the half-width during the 100-ms current pulse is significantly longer than that during the 10- or 50-ms pulse (ANOVA, Bonferroni's multiple-comparisons test). *C*: prolonged depolarizations elicited by 5-Hz, 10-s trains with 10-, 50-, or 100-ms current-pulse duration. As the pulses are made longer, the depolarization becomes smaller. *D*: summary graph of prolonged depolarization amplitude as a function of train current-pulse duration. Depolarization triggered by 10-ms pulses is significantly larger than that evoked by 100-ms pulses, but not 50-ms pulses (ANOVA, Bonferroni's multiple-comparisons test). That said, there is a significant linear trend for a decrease in depolarization amplitude with an increase in pulse duration ( $P < 0.03$ ).

tential (TRP) channels were also tested: 2APB, SKF-96365, MDL-123302A, and  $Gd^{3+}$ . Neurons were held at  $-60$  mV and given the standard voltage stimulus. Separate neurons were used for control and drug delivery. Both  $Gd^{3+}$  and SKF-96365 block voltage-gated  $Ca^{2+}$  channels in bag cell neurons (Hung and Magoski, unpublished observations); therefore all drugs were perfused immediately after the train to eliminate possible side effects on  $Ca^{2+}$  channels. SKF-96365 and 2-APB are best known as antagonists of store-operated  $Ca^{2+}$  influx, including that of bag cell neurons (Arakawa et al. 2000; Baba et al. 2003; Cabello and Schilling 1993; Cordova et al. 2003; Daly et al. 1995; Kachoei et al. 2006; Merritt et al. 1990; Prakriya and Lewis 2001; Tozzi et al. 2003). Addition of 50 or 300  $\mu M$  2-APB did not incur effects that were different from control on peak  $I_{PD}$  ( $-11.6 \pm 2.9$  vs.  $-14.2 \pm 3.5$  or  $-13.0 \pm 5.8$  pA;  $n$  values of 13, 6, and 6; ANOVA, Bonferroni's multiple-comparisons test, not significant). Similarly, 20  $\mu M$  SKF-96365 did not significantly alter peak  $I_{PD}$  compared with control ( $-48.5 \pm 8.2$  vs.  $-48.9 \pm 13.2$  pA;  $n$  values of 10 and 10; unpaired  $t$ -test, not significant). However, MDL-123302A,

a drug recently found to block cation channels (Tahvildari et al. 2004; Van Rossum et al. 2000), appeared to decrease peak  $I_{PD}$  ( $n = 8$ ), but this approached significance only when compared with control ( $n = 10$ ) (Fig. 10A). Finally, 100  $\mu M$   $Gd^{3+}$  ( $n = 8$ ), a classic cation channel blocker (Chakfe and Bourque 2000; Franco and Lansman 1990; Popp et al. 1993; Yang and Sachs 1989), significantly attenuated  $I_{PD}$  amplitude versus control ( $n = 9$ ) (Fig. 10B). In part, these data support the conclusion that a nonselective cation channel may underlie generation of the prolonged depolarization.

#### DISCUSSION

The triggering of a prolonged depolarization by a brief stimulus increases the likelihood of further activity and renders a neuron more sensitive to subsequent inputs. Whim and Kaczmarek (1998) found that delivering 20 action potentials at 1 Hz to *Aplysia* bag cell neurons generated a depolarizing afterpotential that lasted several minutes. The prolonged depolarization examined in the present study was

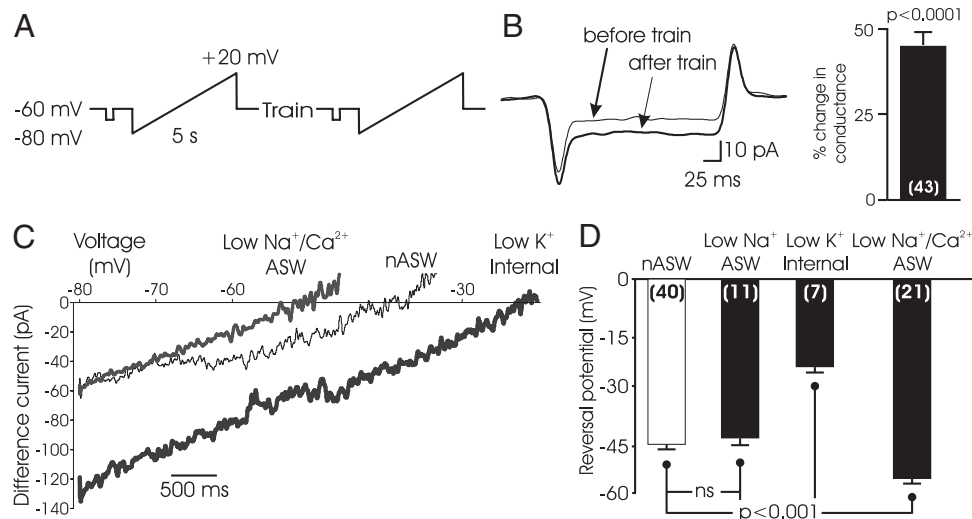


FIG. 8.  $I_{PD}$  properties are consistent with a nonselective cation channel. **A**: ramp protocol for testing the reversal potential. Neurons are voltage clamped at  $-60$  mV and given a 200-ms prepulse to  $-70$  mV to determine conductance. A 5-s ramp from  $-80$  to  $+20$  mV is given before and after  $I_{PD}$  is generated by the standard voltage train. Difference current is then calculated by subtracting the current before the train from the current after the train. **B**, *left*: sample traces of the current during the  $-70$ -mV test pulse denoting the increase in conductance before and after the train. *Right*: summary graph of the percentage change in conductance. There is a significant increase in conductance after the train, suggesting that channels open during  $I_{PD}$ . A one-sample *t*-test finds this change in conductance to be significantly different from zero. **C**: examples of current-voltage relationships calculated from the ramp protocol in the presence of 3 different ionic conditions: nASW (thin line), lowered internal  $K^+$  (thick line), and lowered external  $Na^+/Ca^{2+}$  (medium line). Outward current is truncated because as the voltage approached 0 mV, large, voltage-gated  $K^+$  current would sometimes contaminate the trace. **D**: summary bar graph of the reversal potentials for nASW, low external  $Na^+$ , low internal  $K^+$ , and low external  $Na^+$  and  $Ca^{2+}$ . Lowering external  $Na^+$  does not shift the reversal potential; however, lowering external  $Na^+$  and  $Ca^{2+}$  or lowering internal  $K^+$  concentrations significantly shifts the reversal potential leftward and rightward, respectively (ANOVA, Bonferroni's multiple-comparisons test).

observed in the same neurons, although it was generated using a 5-Hz, 10-s stimulus and was both larger and longer. A stimulation of 4–6 Hz at 10 s is in fact commonly used to evoke the afterdischarge in intact bag cell neurons clusters (Fisher et al. 1994; Kaczmarek et al. 1982; Magoski and

Kaczmarek 2005; Zhang et al. 2002). It is likely that the prolonged depolarization seen here is the same as, or at least a more robust version of, the depolarizing afterpotential documented by Whim and Kaczmarek (1998). Our data suggest that an optimal level of  $Ca^{2+}$  influx activates cal-

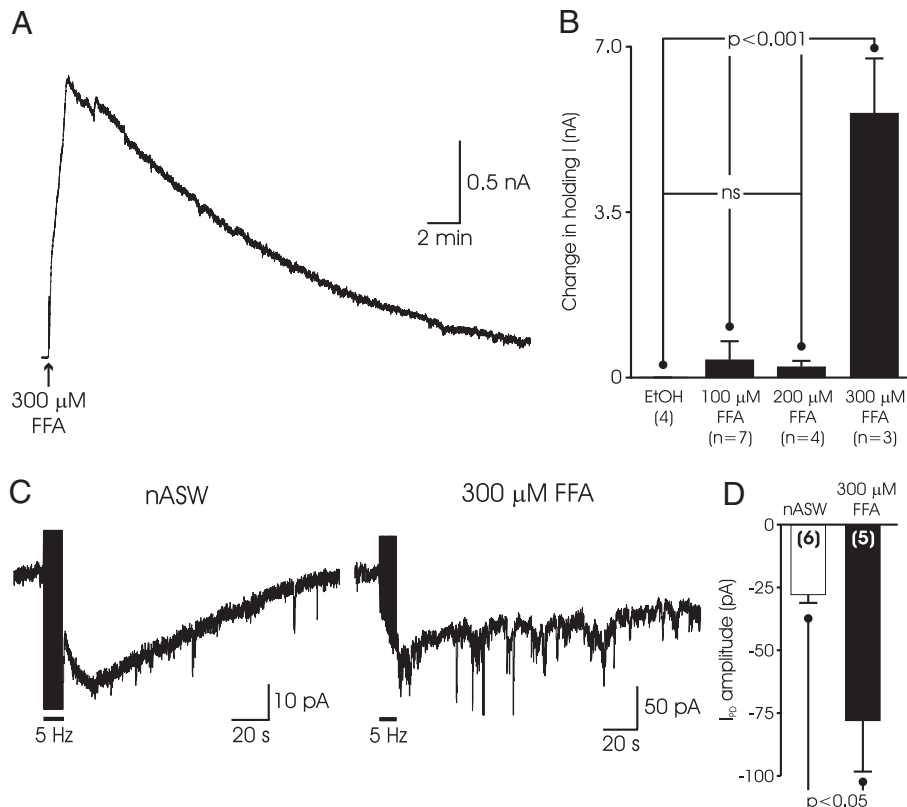


FIG. 9. Flufenamic acid (FFA) increase holding current and  $I_{PD}$ . **A**: lengthy trace depicting the effects of 300  $\mu$ M FFA on holding current under whole cell, voltage clamp at  $-60$  mV. After the addition of FFA, a large outward current develops, which gradually (about 30 min) returns to baseline. **B**: summary graph depicting the effects of 100, 200, and 300  $\mu$ M FFA on holding current compared with 0.07% ethanol (the vehicle). Lower concentrations of FFA do not have significant effects on holding current compared with control; however, 300  $\mu$ M FFA significantly increases the holding current (ANOVA, Bonferroni's multiple-comparisons test). **C**: traces of  $I_{PD}$  while holding at  $-60$  mV in nASW or 300  $\mu$ M FFA after the outward current has subsided. Note that the scale bars are different for the 2 traces and separate neurons are used for control and drug application. Rapid, transient inward currents seen throughout FFA are typical for this drug. **D**: summary graph of nASW vs. 300  $\mu$ M FFA on  $I_{PD}$ . FFA significantly increases  $I_{PD}$  compared with control (unpaired *t*-test).

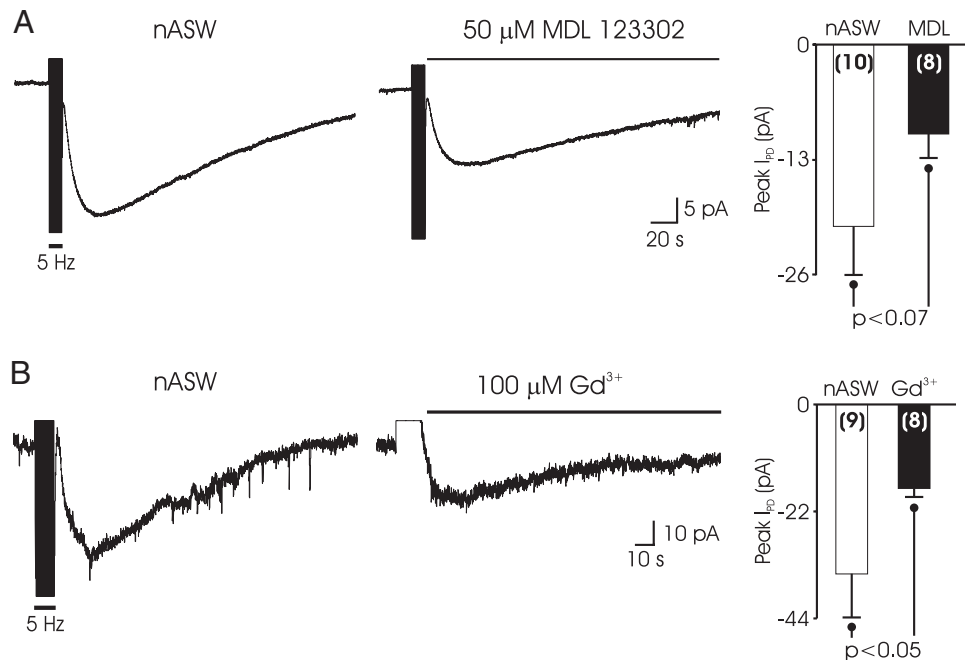


FIG. 10.  $I_{PD}$  is blocked by a classical cation channel antagonist. Both drugs are applied (at bar) immediately after the standard stimulus because of possible effects on voltage-gated  $Ca^{2+}$  currents that would confound the assay if applied earlier. Separate neurons are used for control and drug application. *A, left:* traces of  $I_{PD}$  after perfusion of either nASW or 50  $\mu$ M *cis-N*-(2-phenylcyclopentyl)-azacyclotridec-1-en-2-amine hydrochloride (MDL-123302A or, simply, MDL). *Right:* summary graph comparing the effect of control to MDL on peak  $I_{PD}$  amplitude. Decrease in MDL is not quite significant (unpaired, one-tailed *t*-test). *B, left:*  $I_{PD}$  traces with nASW or with addition of 100  $\mu$ M  $Gd^{3+}$ . *Right:* summary graph noting that  $Gd^{3+}$  significantly reduces peak  $I_{PD}$  compared with control (unpaired, one-tailed *t*-test).

modulin kinase and a voltage-independent, nonselective cation channel to initiate the prolonged depolarization.

The prolonged depolarization in sharp-electrode current clamp lasted for many minutes, whereas  $I_{PD}$  recorded under whole cell voltage clamp usually lasted 3–5 min. Given that the same 5-Hz, 10-s stimulus was delivered in both cases, and there is an increase in conductance in voltage clamp,  $I_{PD}$  is likely the current responsible for the prolonged depolarization. The discrepancy in length may be explained by differences in recording methods. Because whole cell recording allows for fluid exchange between the electrode and the cell, it may have diluted down components required for  $I_{PD}$  generation, thus shortening the duration. Nevertheless, sharp-electrode recording has limitations. Whim and Kaczmarek (1998) used sharp-electrode, switching voltage-clamp to measure inward current after their stimulus. However, that method does not always allow for rapid voltage changes to be accurately clamped. In the voltage-clamp portion of their study, Whim and Kaczmarek (1998) used a train of unclamped action potentials as the stimulus, indicating that, unlike the present study, control over both voltage and the extent of  $Ca^{2+}$  influx was poor.

Whim and Kaczmarek (1998) found that  $Ca^{2+}$  influx was necessary for the response, as have many studies on prolonged depolarizations and plateau potentials (Egorov et al. 2002; Fraser and MacVicar 1996; Morriset and Nagy 1999; Pierson et al. 2005; Rekling and Feldman 1997). Also, the slow onset and lengthy duration of the prolonged depolarization suggests involvement of a second-messenger cascade. Calmodulin is a ubiquitous  $Ca^{2+}$ -binding protein known to regulate ion channels (Levitan 1999; Saimi and Kung 1994); moreover, calmodulin can activate calmodulin kinase (Hanson and Shulman 1992). To test whether this enzyme had a role in the bag cell neuron prolonged depolarization, the calmodulin kinase antagonists KN-62 and CBD were used. The response was significantly attenuated by KN-62, which also blocks short-term facilitation of *Aplysia* sensorimotor synapses at the same concentration used here (Nakanishi et al. 1997). CBD, which

blocks  $Ca^{2+}$ -activation of other bag cell neuron ion channels (Lupinsky and Magoski 2006), was also effective. Other calmodulin antagonists tested included calmidazolium, trifluoperazine, and chlorpromazine. (DeReimer et al. 1984, 1985) found these agents to both block bag cell neuron calmodulin kinase in a biochemical assay and abolish afterdischarges from intact bag cell clusters monitored through extracellular recording. However, when used with cultured neurons, these drugs caused cell detachment and death. Although this has not been observed in *Aplysia* until now, calmidazolium, chlorpromazine, and trifluoperazine all inhibit cell adhesion molecules (Bouillon and Audette 1994; Connor et al. 1981; Cornwell et al. 1983; Lapetina et al. 1986; Liu et al. 2002; Mohri et al. 1998; Sinozara et al. 2001; Soong and Cintron 1985; Weissmann et al. 1986).

TEA, a general  $K^{+}$  channel blocker (Hagiwara and Saito 1959), readily produced very broad action potentials in bag cell neurons, yet strongly attenuated the prolonged depolarization. Similarly, evoking slightly broader action potentials, although not a broad as seen in TEA, by using long current pulses resulted in smaller prolonged depolarizations. There may exist an optimal level of  $Ca^{2+}$  for prolonged depolarization generation and the large  $Ca^{2+}$  influx that occurs during the broad action potentials surpasses this limit. Too much  $Ca^{2+}$  could promote  $Ca^{2+}$  action further away from the membrane and recruit additional calmodulin-dependent proteins, such as a phosphatase, that may inhibit  $I_{PD}$ . This concept was reinforced by our voltage-clamp experiments to determine the most suitable pulse duration. The 100-ms pulse was found to be optimal, despite greater  $Ca^{2+}$  influx at longer durations. That said, if some  $Ca^{2+}$ /calmodulin binding occurs, even at a low level of  $Ca^{2+}$ , it could account for the small, yet ever present occurrence of  $I_{PD}$  at all durations. Brown and Bourque (2004) described a similar phenomenon in magnocellular neurons, where increasingly strong stimulation caused ever greater inhibition of subsequent depolarizing afterpotentials. A  $Ca^{2+}$

window or  $\text{Ca}^{2+}$  limit would ensure specificity and selectivity to incoming stimuli.

The approximately  $-45$  mV reversal potential of  $I_{\text{PD}}$  suggests a nonselective cation current (Partridge and Swandulla 1988). Appropriately, lowering internal  $\text{K}^+$  right-shifted the reversal potential, whereas lowering both external  $\text{Na}^+$  and  $\text{Ca}^{2+}$  caused a left-shift. Surprisingly, lowering external  $\text{Na}^+$  alone produced no change.  $\text{Na}^+$  and  $\text{Ca}^{2+}$  may compete for access to the channel, as is the case for squid voltage-gated  $\text{Na}^+$  current (Chandler and Meves 1965). When only external  $\text{Na}^+$  was lowered,  $\text{Ca}^{2+}$  would become the dominant permeant ion and prevent a shift in reversal potential. The voltage-independent cation current activated by intracellular  $\text{Ca}^{2+}$  release in bag cell neurons, reported by Knox et al. (1996), may be responsible for  $I_{\text{PD}}$ . However, keeping in mind that those authors used sharp-electrode and not whole cell voltage clamp, the Knox et al. (1996) current reverses at about  $-20$  mV.  $I_{\text{PD}}$  most likely conducts more  $\text{K}^+$  than  $\text{Na}^+$  and may pass  $\text{Ca}^{2+}$ . Activity- or  $\text{Ca}^{2+}$ -dependent, nonvoltage-gated cation currents, which reverse between 0 and  $-50$  mV, mediate depolarizing afterpotentials, prolonged depolarizations, plateau potentials, or afterdischarges in *Aplysia* L2–L6 (Kramer and Zucker 1985), crab somatogastric ganglion (Zhang et al. 1995), *Helix pomatia* pacemaker (Swandulla and Lux 1985), septal nucleus (Hasuo et al. 1990), nuclei basalis (Tatsumi and Katayama 1994), prefrontal cortical (Haj-Dahmane and Andrade 1997, 1999), hippocampal cortical (Fraser and MacVicar 1996), supraoptic nucleus (Brown and Bourque 2004), dorsal horn (Morrisset and Nagy 1999), and entorhinal cortical (Tahvildari et al. 2004) neurons.

Of the antagonists,  $I_{\text{PD}}$  was blocked only by  $\text{Gd}^{3+}$ , a well-established nonselective cation channel blocker at  $10$ – $200$   $\mu\text{M}$  (Breneton et al. 2001; Chakfe and Bourque 2000; Formenti et al. 2001; Giannone et al. 2000; Ohki et al. 2000; Smith et al. 2004; Wagner et al. 2000; Xiong et al. 1997; Zitt et al. 1997). Regarding TTX, although it is most commonly known as a  $\text{Na}^+$  channel blocker (Narahashi et al. 1964), it was tested here because  $100$   $\mu\text{M}$  was found to block a voltage-dependent cation channel in bag cell neurons (Wilson et al. 1996). Because TTX did not affect  $I_{\text{PD}}$  and the current–voltage relationship was linear, an alternative cation channel is likely involved. In addition to  $\text{Gd}^{3+}$ , the store-operated  $\text{Ca}^{2+}$  current blockers 2-APB and SKF-96365 (Arakawa et al. 2000; Baba et al. 2003; Merritt et al. 1990; Prakriya and Lewis 2001) were also previously used to block cation channels, including TRP channels, at  $20$ – $100$   $\mu\text{M}$  (Bengtson et al. 2004; Gee et al. 2003; Kim et al. 2003; Tahvildari et al. 2004; Tozzi et al. 2003; Van Rossum et al. 2000). Recently, Kachoei et al. (2006) found that both 2-APB and SKF-96365 blocked store-operated  $\text{Ca}^{2+}$  influx in bag cell neurons. This store-operated channel appears to be distinct from  $I_{\text{PD}}$ . Finally, MDL-123302A was first recognized as an adenylate cyclase antagonist (Siegel and Wiech 1976), but has since been used to block cation channels at  $10$ – $100$   $\mu\text{M}$  (Gee et al. 2003; Tahvildari et al. 2004; Van Rossum et al. 2000). The inhibitory effects of this drug on  $I_{\text{PD}}$  approached significance. A  $\text{Gd}^{3+}$ -sensitive, voltage-independent, nonselective cation channel is likely involved in  $I_{\text{PD}}$  generation.

FFA, the classic cation channel blocker, is commonly used at a concentration of  $100$ – $500$   $\mu\text{M}$  (Bengtson et al. 2004; Ghamari-Langroudi and Bourque 2002; Haj-Dahmane and

Andrade 1999; Morrisset and Nagy 1999; Partridge and Valenzuela 2000; Shaw et al. 1995). FFA did not block  $I_{\text{PD}}$ , which is not entirely unique, as a TRP-type cation channel in rat heart is blocked by  $\text{Gd}^{3+}$  but not FFA (Ohki et al. 2000). In bag cell neurons,  $300$   $\mu\text{M}$  FFA generated a large outward current and increased  $I_{\text{PD}}$  amplitude. FFA can stimulate leak-type  $\text{K}^+$  channels (Takahira et al. 2005) and the outward current in bag cell neurons is likely a result of  $\text{K}^+$  efflux (Gardam and Magoski, unpublished observation). FFA may also be activating  $I_{\text{PD}}$ , as it does for some TRP channels (Hill et al. 2006; Warren et al. 2006). Alternatively, FFA could potentiate  $I_{\text{PD}}$  by releasing  $\text{Ca}^{2+}$  from internal stores, as is the case for *Helix* and hippocampal neurons (Partridge and Valenzuela 2000; Shaw et al. 1995). Our data imply that when using FFA, possible secondary effects should be taken into account.

The prolonged depolarization greatly outlasts the initial stimulus and could contribute to the afterdischarge in vivo. In the intact cluster, a brief presynaptic stimulus to the electrically coupled bag cell neurons initiates a nearly 30-min afterdischarge and release of egg-laying hormone (Conn and Kaczmarek 1989; Kaczmarek et al. 1979; Kupfermann and Kandel 1970). Mayeri et al. (1979b) suggested that excitation could spread from a few cells to the rest of the cluster after selective stimulation of synaptic inputs to individual bag cell neurons. Prolonged depolarizations in a small number of neurons could, in part, support the start of the afterdischarge. Additional mechanisms would come into play later on, including direct  $\text{Ca}^{2+}$ /calmodulin- and protein kinase C-dependent activation of the aforementioned voltage-dependent cation channel (Lupinsky and Magoski 2006; Magoski 2004; Magoski and Kaczmarek 2005; Magoski et al. 2002; Wilson et al. 1996, 1998). This current is larger than  $I_{\text{PD}}$  and the two would sum to provide the necessary long-term depolarizing drive for the afterdischarge.

Parallels can be drawn between the prolonged depolarization and similar phenomena in other neurons, where long-term changes to excitability occur after activity. For example, in rodent magnocellular, rostral ambiguous, dorsal horn, and entorhinal cortex neurons, a brief stimulus results in very long or even persistent depolarizations and/or spiking (Andrew and Dudek 1983; Egorov et al. 2002; Morrisset and Nagy 1999; Rekling and Feldman 1997). Some brain areas displaying these excitability changes are responsible for learning, memory, and motivation. Thus activity-dependent changes in excitability appear crucial for the initiation of fundamental behaviors, such as reproduction, as well as more complex nervous system functions.

#### REFERENCES

- Andrew RD, Dudek FE. Burst discharge in mammalian neuroendocrine cells involves an intrinsic regenerative mechanism. *Science* 221: 1050–1052, 1983.
- Aracri P, Colombo E, Mantegazza M, Scalmani P, Curia G, Avanzini G, Franceschetti S. Layer-specific properties of the persistent sodium current in sensorimotor cortex. *J Neurophysiol* 95: 3460–3468, 2006.
- Arakawa N, Sakaue M, Yokoyama I, Hashimoto H, Koyama Y, Baba A, Matsuda T. KB-R7943 inhibits store-operated  $\text{Ca}^{2+}$  entry in cultured neurons and astrocytes. *Biochem Biophys Res Commun* 279: 354–357, 2000.
- Arch S. Biosynthesis of the egg-laying hormone (ELH) in the bag cell neurons of *Aplysia californica*. *J Gen Physiol* 60: 102–119, 1972.

- Baba A, Yasui T, Fujisawa S, Yamada RX, Yamada MK, Nishiyama N, Matsuki N, Ikegaya Y. Activity-evoked capacitative  $Ca^{2+}$  entry: implications in synaptic plasticity *J Neurosci* 23: 7737–7741, 2003.
- Bengtson CP, Tozzi A, Bernardi G, Mercuri NB. Transient receptor potential-like channels mediate metabotropic glutamate receptor EPSCs in rat dopamine neurons. *J Physiol* 555: 323–330, 2004.
- Blankenship JE, Haskins JT. Electrotonic coupling among neuroendocrine cells in *Aplysia*. *J Neurophysiol* 42: 347–355, 1979.
- Bouillon M, Audette M. Retinoic acid-stimulated intercellular adhesion molecule-1 expression on SK-N-SH cells: calcium/calmodulin-dependent pathway. *Cancer Res* 54: 4144–4149, 1994.
- Brown CH, Bourque CW. Autocrine feedback inhibition of plateau potentials terminates phasic bursts in magnocellular neurosecretory cells of the rat supraoptic nucleus. *J Physiol* 557: 949–960, 2004.
- Brown RO, Mayeri E. Positive feedback by autoexcitatory neuropeptides in neuroendocrine bag cells of *Aplysia*. *J Neurosci* 9: 1443–1451, 1989.
- Cabello OA, Schilling WP. Vectorial  $Ca^{2+}$  flux from the extracellular space to the endoplasmic reticulum via a restricted cytoplasmic compartment regulates inositol 1,4,5-trisphosphate-stimulated  $Ca^{2+}$  release from internal stores in vascular endothelial cells. *Biochem J* 295: 357–366, 1993.
- Chakfe Y, Bourque CW. Excitatory peptides and osmotic pressure modulate mechanosensitive cation channels in concert. *Nat Neurosci* 3: 572–579, 2000.
- Chandler WK, Meves H. Voltage clamp experiments on internally perfused giant axons. *J Physiol* 180: 788–820, 1965.
- Chiu AY, Hunkapiller MW, Heller E, Stuart DK, Hood LE, Strumwasser F. Purification and primary structure of the neuropeptide egg-laying hormone of *Aplysia californica*. *Proc Natl Acad Sci USA* 76: 6656–6660, 1979.
- Conn PJ, Kaczmarek LK. The bag cell neurons of *Aplysia*. A model for the study of the molecular mechanisms involved in the control of prolonged animal behaviors. *Mol Neurobiol* 3: 237–273, 1989.
- Connor CG, Brady RC, Brownstein BL. Trifluoperazine inhibits spreading and migration of cells in culture. *J Cell Physiol* 108: 299–307, 1981.
- Cordova D, Delpech VR, Satelle DB, Rauh JJ. Spatiotemporal calcium signaling in a *Drosophila melanogaster* cell line stably expressing a *Drosophila* muscarinic acetylcholine receptor. *Invert Neurosci* 5: 19–28, 2003.
- Cornwell MM, Juliano RL, Davies PJ. Inhibition of the adhesion of Chinese hamster ovary cells by the naphthylsulfonamides dansylcadaverine and N-(6-aminoethyl)-5-chloro-1-naphthylsulfonamide (W7). *Biochim Biophys Acta* 762: 414–419, 1983.
- Daly JW, Leuders J, Padgett WL, Shin Y, Gusovsky F. Malotoxin-elicited calcium influx in cultured cells. *Biochem Pharmacol* 50: 1187–1197, 1995.
- Dembrow NC, Jing J, Brezina V, Weiss KR. A specific synaptic pathway activates a conditional plateau potential underlying protraction phase in the *Aplysia* feeding central pattern generator. *J Neurosci* 24: 5230–5238, 2004.
- DeRiemer SA, Kaczmarek LK, Lai Y, McGuinness TL, Greengard P. Calcium/calmodulin-dependent protein phosphorylation in the nervous system of *Aplysia*. *J Neurosci* 4: 1618–1625, 1984.
- DeRiemer SA, Schweitzer B, Kaczmarek LK. Inhibitors of calcium-dependent enzymes prevent the onset of afterdischarge in the peptidergic bag cell neurons of *Aplysia*. *Brain Res* 340: 175–180, 1985.
- Derjean D, Bertrand S, Nagy F, Shefchyk SJ. Plateau potentials and membrane oscillations in parasympathetic preganglionic neurons and intermediolateral neurons in the rat lumbosacral spinal cord. *J Physiol* 563: 583–596, 2005.
- Dudek FE, Cobbs JS, Pinsker HM. Bag cell electrical activity underlying spontaneous egg laying in freely behaving *Aplysia brasiliana*. *J Neurophysiol* 42: 804–817, 1979.
- Egorov AV, Hamam BN, Fransén E, Hasselmo ME, Alonso AA. Graded persistent activity in entorhinal cortex neurons. *Nature* 420: 173–178, 2002.
- Eyzaguirre C, Kuffler SW. Further study of soma, dendrite, and axon excitation in single neurons. *J Gen Physiol* 39: 121–153, 1955.
- Fisher TE, Levy S, Kaczmarek LK. Transient changes in intracellular calcium associated with a prolonged increase in excitability in neurons of *Aplysia californica*. *J Neurophysiol* 71: 1254–1257, 1994.
- Formenti A, DeSimoni A, Arrigoni E, Martina M. Changes in extracellular  $Ca^{2+}$  can affect the pattern of discharge in rat thalamic neurons. *J Physiol* 535: 33–45, 2001.
- Franco A Jr, Lansman JB. Stretch-sensitive channels in developing muscle cells from a mouse cell line. *J Physiol* 427: 361–380, 1990.
- Fraser DD, MacVicar BA. Cholinergic-dependent plateau potential in hippocampal CA1 pyramidal neurons. *J Neurosci* 16: 4113–4128, 1996.
- Gee CE, Benquet P, Gerber U. Group I metabotropic glutamate receptors activate a calcium-sensitive transient receptor potential-like conductance in rat hippocampus. *J Physiol* 546: 655–664, 2003.
- Ghamari-Langroudi M, Bourque CW. Flufenamic acid blocks depolarizing afterpotentials and phasic firing in rat supraoptic neurons. *J Physiol* 545: 537–542, 2002.
- Giannone G, Takeda K, Kleschyov AL. Novel activation of non-selective cationic channels by dinitrosyl iron-thiosulfate in PC12 cells. *J Physiol* 529: 735–745, 2000.
- Hagiwara S, Saito N. Voltage-current relations in nerve cell membrane of *Onchidium verruculatum*. *J Physiol* 148: 161–179, 1959.
- Haj-Damane S, Andrade R. Calcium-activated cation nonselective current contributes to the fast afterdepolarization in rat prefrontal cortex neurons. *J Neurophysiol* 78: 1983–1989, 1997.
- Haj-Damane S, Andrade R. Muscarinic receptors regulate two different calcium-dependent non-selective cation currents in rat prefrontal cortex. *Eur J Neurosci* 11: 1973–1980, 1999.
- Hanson PI, Schulman H. Neuronal  $Ca^{2+}$ /calmodulin-dependent protein kinases. *Annu Rev Biochem* 61: 559–601, 1992.
- Hasuo H, Phelan KD, Twery MJ, Gallagher JP. A calcium-dependent slow afterdepolarization recorded in rat dorsolateral septal nucleus neurons in vitro. *J Neurophysiol* 64: 1838–1846, 1990.
- Hill AJ, Hinton JM, Cheng H, Gao Z, Bates DO, Hancox JC, Langton PD, James AF. A TRPC-like non-selective cation current activated by  $\alpha$ 1-adrenoceptors in rat mesenteric artery smooth muscle cells. *Cell Calcium* 40: 29–40, 2006.
- Hille B. *Ionic Channels of Excitable Membranes*. Sunderland, MA: Sinauer Associates, 2001.
- Kachoei BA, Knox RJ, Uthuz D, Levy S, Kaczmarek LK, Magoski NS. A store-operated  $Ca^{2+}$  influx pathway in the bag cell neurons of *Aplysia*. *J Neurophysiol* 96: 2688–2698, 2006.
- Kaczmarek LK, Finbow M, Revel JP, Strumwasser F. The morphology and coupling of *Aplysia* bag cells within the abdominal ganglion and in cell culture. *J Neurobiol* 10: 535–550, 1979.
- Kaczmarek LK, Jennings KR, Strumwasser F. An early sodium and a late calcium phase in the afterdischarge of peptide-secreting neurons of *Aplysia*. *Brain Res* 238: 105–115, 1982.
- Kim SJ, Kim YS, Yuan JP, Petralia RS, Worley PF, Linden DJ. Activation of the TRPC1 cation channel by metabotropic glutamate receptor mGluR1. *Nature* 426: 285–291, 2003.
- Klein M, Kandel ER. Presynaptic modulation of voltage-dependent  $Ca^{2+}$  current: mechanism for behavioral sensitization in *Aplysia californica*. *Proc Natl Acad Sci USA* 75: 3512–3516, 1978.
- Knox RJ, Jonas EA, Kao LS, Smith PJ, Connor JA, Kaczmarek LK.  $Ca^{2+}$  influx and activation of a cation current are coupled to intracellular  $Ca^{2+}$  release in peptidergic neurons of *Aplysia californica*. *J Physiol* 494: 627–639, 1996.
- Kramer RH, Zucker RS. Calcium-dependent inward current in *Aplysia* bursting pace-maker neurons. *J Physiol* 362: 107–130, 1985.
- Kupfermann I. Stimulation of egg laying: possible neuroendocrine function of bag cells of abdominal ganglion of *Aplysia californica*. *Nature* 216: 814–815, 1967.
- Kupfermann I. Stimulation of egg laying by extracts of neuroendocrine cells (bag cells) of abdominal ganglion of *Aplysia*. *J Neurophysiol* 33: 877–881, 1970.
- Kupfermann I, Kandel ER. Electrophysiological properties and functional interconnections of two symmetrical neurosecretory clusters (bag cells) in abdominal ganglion of *Aplysia*. *J Neurophysiol* 33: 865–876, 1970.
- Lapetina EG, Reep B, Read NG, Moncada S. Adhesion of human platelets to collagen in the presence of prostacyclin, indomethacin and compound BW 755C. *Thromb Res* 41: 325–335, 1986.
- Levitan IB. It is calmodulin after all! Mediator of the calcium modulation of multiple ion channels. *Neuron* 22: 645–648, 1999.
- Li Z, Miyata S, Hatton GI. Inositol 1,4,5-trisphosphate-sensitive  $Ca^{2+}$  stores in rat supraoptic neurons: involvement in histamine-induced enhancement of depolarizing afterpotentials. *Neuroscience* 93: 667–674, 1999.
- Liu J, Chen T, Yu B, Xu Q. Ruscogenin glycoside (Lm-3) isolated from *Liriope muscari* inhibits lymphocyte adhesion to extracellular matrix. *J Pharm Pharmacol* 54: 959–965, 2002.
- Lo FS, Erzurumlu RS. L-type calcium channel-mediated plateau potentials in barrelette cells during structural plasticity. *J Neurophysiol* 88: 794–801, 2002.

- Lupinsky DA, Magoski NS.**  $\text{Ca}^{2+}$ -dependent regulation of a non-selective cation channel from *Aplysia* bag cell neurones. *J Physiol* 575: 491–508, 2006.
- Magoski NS.** Regulation of an *Aplysia* bag-cell neuron cation channel by closely associated protein kinase A and a protein phosphatase. *J Neurosci* 24: 6833–6841, 2004.
- Magoski NS, Kaczmarek LK.** Association/dissociation of a channel-kinase complex underlies state-dependent modulation. *J Neurosci* 25: 8037–8047, 2005.
- Magoski NS, Knox RJ, Kaczmarek LK.** Activation of a  $\text{Ca}^{2+}$ -permeable cation channel produces a prolonged attenuation of intracellular  $\text{Ca}^{2+}$  release in *Aplysia* bag cell neurones. *J Physiol* 522: 271–283, 2000.
- Magoski NS, Wilson GF, Kaczmarek LK.** Protein kinase modulation of a neuronal cation channel requires protein–protein interactions mediated by an Src homology 3 domain. *J Neurosci* 22: 1–9, 2002.
- Mayeri E, Brownell P, Branton WD.** Multiple, prolonged actions of neuroendocrine bag cells on neurons in *Aplysia*. II. Effects on beating pacemaker and silent neurons. *J Neurophysiol* 42: 1185–1197, 1979b.
- Mayeri E, Brownell P, Branton WD, Simon SB.** Multiple, prolonged actions of neuroendocrine bag cells on neurons in *Aplysia*. I. Effects on bursting pacemaker neurons. *J Neurophysiol* 42: 1165–1184, 1979a.
- Mercer AR, Kloppenburg P, Hildebrand JG.** Plateau potentials in developing antennal-lobe neurons of the moth, *Manduca sexta*. *J Neurophysiol* 93: 1949–1958, 2005.
- Merritt JE, Armstrong WP, Benham CD, Hallam TJ, Jacob R, Jaxa-Chamiec A, Leigh BK, McCarthy SA, Moorees KE, Rink TJ.** SK&F 96365, a novel inhibitor of receptor-mediated calcium entry. *Biochem J* 271: 515–522, 1990.
- Mohri T, Kameshita I, Suzuki S, Hioki K, Tokunaga R, Takatani S.** Rapid adhesion and spread of non-adherent colon cancer Colo201 cells induced by the protein kinase inhibitors, K252a and KT5720 and suppression of the adhesion by the immunosuppressants FK506 and cyclosporin A. *Cell Struct Funct* 23: 255–264, 1998.
- Morisset V, Nagy F.** Ionic basis for plateau potentials in deep dorsal horn neurons of the rat spinal cord. *J Neurosci* 17: 7309–7316, 1999.
- Nakanishi K, Zhang F, Baxter DA, Eskin A, Byrne JH.** Role of calcium-calmodulin-dependent protein kinase II in modulation of sensorimotor synapses in *Aplysia*. *J Neurophysiol* 78: 409–416, 1997.
- Naraghi M, Neher E.** Linearized buffered  $\text{Ca}^{2+}$  diffusion in microdomains and its implications for calculation of  $[\text{Ca}^{2+}]$  at the mouth of a calcium channel. *J Neurosci* 17: 6961–6973, 1997.
- Narahashi T, Moore JW, Scott WR.** Tetrodotoxin blockage of sodium conductance increase in lobster giant axons. *J Gen Physiol* 47: 965–974, 1964.
- Ohki G, Miyoshi T, Murata M, Ishibashi K, Imai M, Suzuki M.** A calcium-activated cation current by an alternatively spliced form of Trp3 in the heart. *J Biol Chem* 275: 39055–39060, 2000.
- Partridge LD, Swandulla D.** Calcium-activated non-specific cation channels. *Trends Neurosci* 11: 69–72, 1988.
- Partridge LD, Valenzuela CF.** Block of hippocampal CAN channels by flufenamate. *Brain Res* 867: 143–148, 2000.
- Payne ME, Fong YL, Ono T, Colbran RJ, Kemp BE, Soderling TR, Means AR.** Calcium/calmodulin-dependent protein kinase II. Characterization of distinct calmodulin binding and inhibitory domains. *J Biol Chem* 263: 7190–7195, 1988.
- Perrier JF, Hounsgaard J.** 5-HT<sub>2</sub> receptors promote plateau potentials in turtle spinal motoneurons by facilitating an L-type calcium current. *J Neurophysiol* 89: 954–959, 2003.
- Pierson PM, Liu X, Raggenbass M.** Suppression of potassium channels elicits calcium-dependent plateau potentials in suprachiasmatic neurons of the rat. *Brain Res* 1036: 50–59, 2005.
- Pinsker HM, Dudek FE.** Bag cell control of egg-laying in freely moving *Aplysia*. *Science* 197: 490–493, 1977.
- Popp R, Englert HC, Lang HJ, Gogelein H.** Inhibitors of nonselective cation channels in cells of the blood-brain barrier. *EXS* 66: 213–218, 1993.
- Prakriya M, Lewis RS.** Potentiation and inhibition of  $\text{Ca}^{2+}$  release-activated  $\text{Ca}^{2+}$  channels by 2-aminoethyl-diphenyl borate (2-APB) occurs independently of IP<sub>3</sub> receptors. *J Physiol* 536: 3–19, 2001.
- Quattrocki EA, Marshall J, Kaczmarek LK.** A *Shab* potassium channel contributes to action potential broadening in peptidergic neurons. *Neuron* 12: 73–86, 1994.
- Rekling JC, Feldman JL.** Calcium-dependent plateau potentials in rostral ambiguous neurons in the newborn mouse brain stem in vitro. *J Neurophysiol* 78: 2483–2492, 1997.
- Rothman BS, Weir G, Dudek FE.** Egg-laying hormone: direct action on the ovitestic of *Aplysia*. *Gen Comp Endocrinol* 52: 134–141, 1983.
- Russell DF, Hartline DK.** Slow active potentials and bursting motor patterns in pyloric network of the lobster, *Panulirus interruptus*. *J Neurophysiol* 48: 914–937, 1982.
- Russo RE, Hounsgaard J.** Burst-generating neurones in the dorsal horn in an *in vitro* preparation of the turtle spinal cord. *J Physiol* 493: 39–54, 1996.
- Saimi Y, Kung C.** Ion channel regulation by calmodulin binding. *FEBS Lett* 350: 155–158, 1994.
- Scheller RH, Jackson JF, McAllister LB, Schwartz JH, Kandel ER, Axel R.** A family of genes that codes for ELH, a neuropeptide eliciting a stereotyped pattern of behaviour in *Aplysia*. *Cell* 28: 707–719, 1982.
- Shaw T, Lee RJ, Partridge D.** Action of diphenylamine carboxylate derivatives, a family of non-steroidal anti-inflammatory drugs on  $[\text{Ca}^{2+}]_i$  and  $\text{Ca}^{2+}$ -activated channels in neurons. *Neurosci Lett* 190: 121–124, 1995.
- Siegel BW, Wiech NL.** RMI 12330A: an inhibitor of cholera toxin induced intestinal hypersecretion which also inhibits adenylate cyclase activity. *Gastroenterology* 70: 937–945, 1976.
- Sierra F, Comas V, Buno W, Macadar O.** Sodium-dependent plateau potentials in electrocytes of the electric fish *Gymnotus carapo*. *J Comp Physiol A Sens Neural Behav Physiol* 191: 1–11, 2005.
- Sigvardt KA, Rothman BS, Brown RO, Mayeri E.** The bag cells of *Aplysia* as a multitransmitter system: identification of alpha bag cell peptide as a second neurotransmitter. *J Neurosci* 6: 803–813, 1986.
- Sinohara Y, Nakajima Y, Nakanishi S.** Glutamate induces focal adhesion kinase tyrosine phosphorylation and actin rearrangement in heterologous mGluR1-expressing CHO cells via calcium/calmodulin signalling. *J Neurochem* 78: 365–373, 2001.
- Smith SM, Bergsman JB, Harata NC, Scheller RH, Tsien RW.** Recordings from single neocortical nerve terminals reveal a nonselective cation channel activated by decreases in extracellular calcium. *Neuron* 41: 243–256, 2004.
- Soong HK, Cintron C.** Different corneal epithelial healing mechanisms in rat and rabbit: role of actin and calmodulin. *Invest Ophthalmol Vis Sci* 26: 838–848, 1985.
- Stuart DK, Chiu AY, Strumwasser F.** Neurosecretion of egg-laying hormone and other peptides from electrically active bag cell neurons of *Aplysia*. *J Neurophysiol* 43: 488–498, 1980.
- Stuart DK, Strumwasser F.** Neuronal sites of action of a neurosecretory peptide, egg-laying hormone in *Aplysia californica*. *J Neurophysiol* 43: 499–519, 1980.
- Swandulla D, Lux HD.** Activation of a non-specific cation conductance by intracellular  $\text{Ca}^{2+}$  elevation in bursting pacemaker neurons of *Helix pomatia*. *J Neurophysiol* 54: 1430–1443, 1985.
- Tahvildari A, Egorov A, Klink R, Alonso A.** Persistent activity in the entorhinal cortex neurons, TRP channels and intracellular calcium stores. Program No. 516.3. 2004 Abstract Viewer/Itinerary Planner. Washington, DC: Society for Neuroscience, 2004, Online.
- Takahira M, Sakurai M, Sakurada N, Sugiyama K.** Fenamates and diltiazem modulate lipid-sensitive mechano-gated 2P domain K<sup>+</sup> channels. *Pflugers Arch* 451: 474–478, 2005.
- Tatsumi H, Katayama Y.** Brief increases in intracellular  $\text{Ca}^{2+}$  activate K<sup>+</sup> current and non-selective cation current in rat nucleus basalis neurons. *Neuroscience* 58: 553–561, 1994.
- Thompson SH, Smith SJ.** Depolarizing afterpotentials and burst production in molluscan pacemaker neurons. *J Neurophysiol* 39: 153–161, 1976.
- Tokumitsu H, Chijiwa T, Hagiwara M, Mizutani A, Terasawa M, Hidaka H.** KN-62, 1-[N,O-bis(5-isoquinolinesulfonyl)-N-methyl-L-tyrosyl]-4-phenylpiperazine, a specific inhibitor of  $\text{Ca}^{2+}$ /calmodulin-dependent protein kinase II. *J Biol Chem* 265: 4315–4320, 1990.
- Tozzi A, Bengtson CP, Longone P, Carignani C, Fusco FR, Bernardi G, Mercuri NB.** Involvement of transient receptor potential-like channels in responses to mGluR-I activation in midbrain dopamine neurons. *Eur J Neurosci* 18: 2133–2145, 2003.
- Van Rossum DB, Patterson RL, Ma HT, Gill DL.**  $\text{Ca}^{2+}$  entry mediated by store depletion, S-nitrosylation, and TRP3 channels. Comparison of coupling and function. *J Biol Chem* 275: 28562–28568, 2000.
- Warren EJ, Allen CN, Brown RL, Robinson DW.** The light-activated signaling pathway in SCN-projecting rat retinal ganglion cells. *Eur J Neurosci* 23: 2477–2487, 2006.
- Weissmann G, Azaroff L, Davidson S, Dunham P.** Synergy between phorbol esters, 1-oleyl-2-acetyl-glycerol, urushiol, and calcium ionophore in eliciting aggregation of marine sponge cells. *Proc Natl Acad Sci USA* 83: 2914–2918, 1986.

- Whim MD, Kaczmarek LK.** Heterologous expression of the Kv3.1 potassium channel eliminates spike broadening and the induction of a depolarizing afterpotential in the peptidergic bag cell neurons. *J Neurosci* 18: 9171–9180, 1998.
- Wilson GF, Magoski NS, Kaczmarek LK.** Modulation of a calcium-sensitive nonspecific cation channel by closely associated protein kinase and phosphatase activities. *Proc Natl Acad Sci USA* 95: 10938–10943, 1998.
- Wilson GF, Richardson FC, Fisher TE, Olivera BM, Kaczmarek LK.** Identification and characterization of a Ca<sup>2+</sup>-sensitive nonspecific cation channel underlying prolonged repetitive firing in *Aplysia* neurons. *J Neurosci* 16: 3661–3671, 1996.
- Xiong ZG, Lu WY, MacDonald JF.** Extracellular calcium sensed by a novel cation channel in hippocampal neurons. *Proc Natl Acad Sci USA* 94: 7012–7017, 1997.
- Xu J, Kang N, Jiang L, Nedergaard M, Kang J.** Activity-dependent long-term potentiation of intrinsic excitability in hippocampal CA1 pyramidal neurons. *J Neurosci* 25: 1750–1760, 2005.
- Yang XC, Sachs F.** Block of stretch-activated ion channels in *Xenopus* oocytes by gadolinium and calcium ions. *Science* 243: 1068–1071, 1989.
- Zhang B, Wootton JF, Harris-Warrick RM.** Calcium-dependent plateau potentials in a crab somatogastric ganglion motor neuron. II. Calcium-activated slow inward current. *J Neurophysiol* 74: 1938–1946, 1995.
- Zhang W, Linden DJ.** The other side of the engram: experience-driven changes in neuronal intrinsic excitability. *Nat Rev Neurosci* 4: 885–900, 2003.
- Zhang Y, Magoski NS, Kaczmarek LK.** Prolonged activation of Ca<sup>2+</sup>-activated K<sup>+</sup> current contributes to the long-lasting refractory period of *Aplysia* bag cell neurons. *J Neurosci* 22: 10134–10141, 2002.
- Zitt C, Obukhov AG, Strubing C, Zobel A, Kalkbrenner F, Luckhoff A, Schultz G.** Expression of TRPC3 in Chinese hamster ovary cells results in calcium-activated cation currents not related to store depletion. *J Cell Biol* 138: 1333–1341, 1997.